THE EFFECTS OF DESICCATION ON SOIL DEFORMATION

by

John D. Wineland

B. S., Kansas University
Lawrence, Kansas
1969

A MASTER'S THESIS

submitted in partial fulfillment of the

requirements for the degree

MASTER OF SCIENCE

Department of Civil Engineering

KANSAS STATE UNIVERSITY
Manhattan, Kansas

1979

Approved by:

Edwin C. Lindly

Major Professor

ACKNOWLEDGEMENTS

The author wishes to express his gratitude and sincere appreciation to the following individuals:

To his wife, Jolene for her sympathy and encouragement, particularly during the writing of the thesis.

To his children, Joel and Amy for sacrificing their time with dad.

To his parents, J. D. and Maxine Wineland for their encouragement in continuing his education.

To the Kansas Department of Transportation and to G. N. Clark in particular for encouraging professional development and making time and money available for implementing the use of modern methods of computer analysis.

To the Federal Highway Administration for their efforts in making advanced technology available and in working out problems which developed in the application of this technology.

To Miss Dolores Galvan for typing the rough drafts of the thesis.

To Mrs. Joan Edwards for typing the final manuscript.

To Mr. Larry Moser for his work in preparing the graphical portions of the thesis.

To Dr. Myron Hayden, who served as principal advisor and to the rest of the committee members, Professor E. C. Lindly, Professor E. R. Russell, and Professor Stanley Clark.

TABLE OF CONTENTS

TABLE OF CONTENTS (Continued)

LIST OF TABLES

LIST OF FIGURES

LIST OF FIGURES (Continued)

CHAPTER I

INTRODUCTION

The increasing use of high earthen embankments, in addition to the proximity of various highway construction projects to underground utilities, has increased the need to accurately predict any soil deformation which is likely to occur. This need is particularly true for soils which have a variable strength profile with depth, as a result of desiccation. Desiccation resulting from the evaporation of the interstitial water, causes the soil near the ground surface to consolidate, thus resulting in the development of a soil profile which decreases in strength with depth. Information gained from this research could aid in both identifying the possible existences of desiccated soils and in properly accounting for their increased strength.

Statement of the Problem

Consolidation is the process whereby a soil mass decreases in volume as a result of the removal of interstitial water. This phenomenon was first described by Terzaghi (1) analytically in 1925. In addition to an analytical analysis, he suggested a laboratory procedure to predict the magnitude of consolidation by applying a vertical stress to a soil sample which is laterally confined.

Highway departments have customarily used consolidation theory to predict settlements in the foundations of earthen embankments. The application of this concept increases in validity as the distance from the embankment toe increases. Thus, under the center of an embankment, the lateral strain in the soil which results from the weight of the embankment is significantly reduced because of the increase in laterally applied stress. The major deformation which is likely to occur near the toe of a slope is a lateral rather than vertical movement of the foundation soil. Experience has shown that, when a foundation soil is soft, the lateral movement in the foundation near the toe of an embankment may be many times larger than the corresponding vertical movement. The relative magnitude of the lateral and vertical displacements which are likely to occur within the foundation soils due to embankment construction is shown conceptually in Figure 1. Therefore, the application of conventional one-dimensional consolidation theory will yield results which are only a fraction of the total deformation.

Adequate determination of the magnitude of soil strain which is likely to occur as a result of the construction of an embankment is important because of the effect it may have on buried structures (i.e., utilities, drainage structures, etc.). For example, a highway recently constructed by the Kansas Department of Transportation crossed over a rural road which had two 16 inch and one 54 inch diameter water lines running parallel to it. These water lines passed under the toe of an embankment used in the bridge approach. Because of the proximity of the buried water lines to the toe of the embankment, accurate estimates of the magnitude of the vertical and lateral strains of the foundation soils had to be made. Failure to make these accurate predictions could have resulted in considerable increase in construction time and costs.

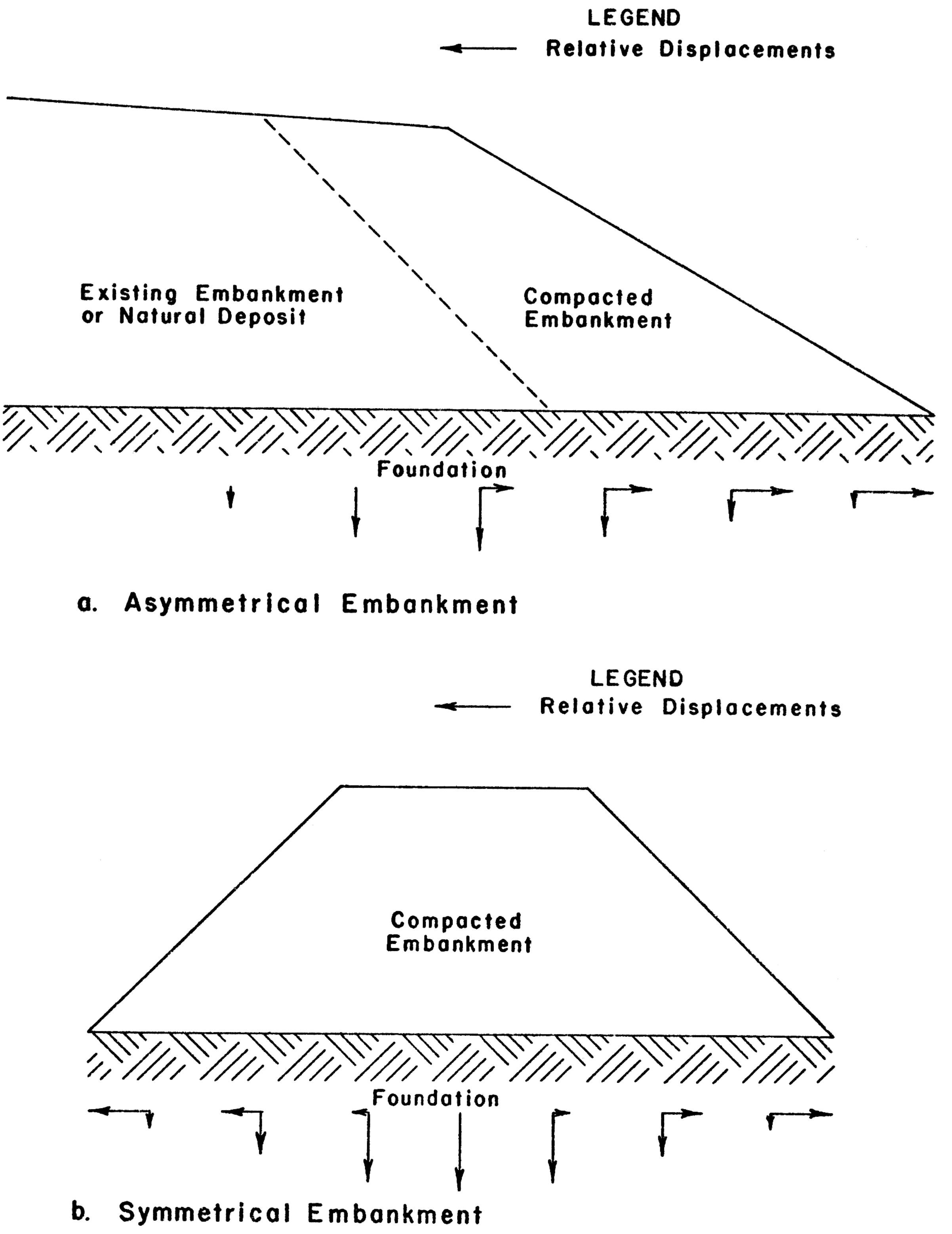

Figure 1. Conceptual Illustration of Relative Displacements Under an Embankment.

As an aid in analyzing this type of problem, the Kansas Department of Transportation obtained a finite element computer program from the Federal Highway Administration. This program, developed by Ozawa and Duncan (2), can be used to analyze the various soil stresses, therefore it serves as a useful tool in stability analysis. Since the program is based on the principles and concepts of the theory of elasticity, it could also be used to predict soil displacements within an embankment. Therefore, this study was conducted in an attempt to implement the use of this finite element program to predict potential movements within the embankment and foundation. Since the program computes the stresses and corresponding strains within a soil mass based on strength parameters, an adequate method of assessing those parameters had to be developed. This is particularly important when the foundation material varies in strength as a result of desiccation.

Scope of Investigation

The scope of this investigation is included in three phases. The first phase was the design and construction of an earthen embankment utilizing conventional design and construction procedures. Also included was the installation of monitoring devices within the embankment to measure pore pressures and movement during and after construction. The second phase consisted of correlating the deflections predicted using the finite element program to those that were actually measured by the field instruments. The results of this correlation indicated that the predicted deflections based upon the finite element program were far in excess of those measured in the field. An investigation was then conducted to determine the reasons for this large discrepancy. The investigation lead to the conclusion that the failure to recognize and account for the increased soil stiffness which resulted from the desiccation of the foundation material was a major factor in this large difference.

The third phase consisted of the development of an adequate means of assessing the strength of a desiccated soil. During this phase the conventional sampling and testing program used to provide the design parameters was examined. Based on this examination, modifications in the previously specified method of sampling and testing were made to improve the quality of the results.

CHAPTER II

A LITERATURE CRITIQUE OF DESICCATION AND RESULTING OVERCONSOLIDATION OF A SOIL

Consolidation of a soil mass is defined as the deformation which results from a change in the relative positions of the soil particles and the corresponding decrease in interstitial volume. This decrease in volume is caused by a change in the interstitial or pore pressure which could occur because of either of the two following conditions: 1) additional load applied to the soil mass, or 2) desiccation of the upper soil strata. Whenever a soil is consolidated more than would be expected from the vertical stress currently applied, a state of overconsolidation exists.

The fact that desiccation of a soil near the ground surface can cause overconsolidation has been known by soils engineers for many years. However, the process of desiccation and its resulting effect on the strength characteristics of a soil are not well understood. It is known that the relative effect of desiccation on a soil is dependent on a number of physical properties (i.e., grain-size, clay content, mineralogical make-up, etc.). Therefore, this chapter will present the current theories used to explain its cause and subsequent effect on the strength parameters of a soil.

Terzaghi and Peck (3) describe the process of desiccation based on the laws of physics. According to their theory, evaporation at the air-water boundary is dependent on both the relative humidity of the ambient air and the surface tension of the water. Since the relative humidity is rarely higher than 95%, evaporation occurs causing negative pore pressure to develop in the soil voids in a manner similar to a capillary tube. Thus the magnitude of the negative pore pressure which develops is dependent upon the size of the voids at the soil surface. They theorized that when the water content decreases below the shrinkage limit, air begins to penetrate the soil and the water withdraws into corners of the voids. This continues until the negative pore pressure increases and a limiting value is reached, after which evaporation ceases.

For water contents above the shrinkage limit, the surface tension induced within the voids produces an effective pressure equal to the negative pore pressure developed. The negative hydrostatic pressure which develops within the voids causes the soil to consolidate. This form of consolidation has been observed to occur up to depths of 20 feet depending on the humidity and frequency of rainfall.

Lambe and Whitman (4) present a graph which they refer to as the relationship of the undrained shear strength to the overconsolidation ratio for an isotropically consolidated weald clay. Such a graph is presented in Figure 2. The graph consists of a ratio of the shear strength of a normally consolidated sample divided by the shear strength determined for a similar sample which is overconsolidated, plotted against the reciprocal of the overconsolidation ratio. The graph illustrates that by reducing the consolidation stress to one half its maximum value, the corresponding reduction in the undrained shear strength is only 17 percent. Thus, for the materials tested, a soil with an

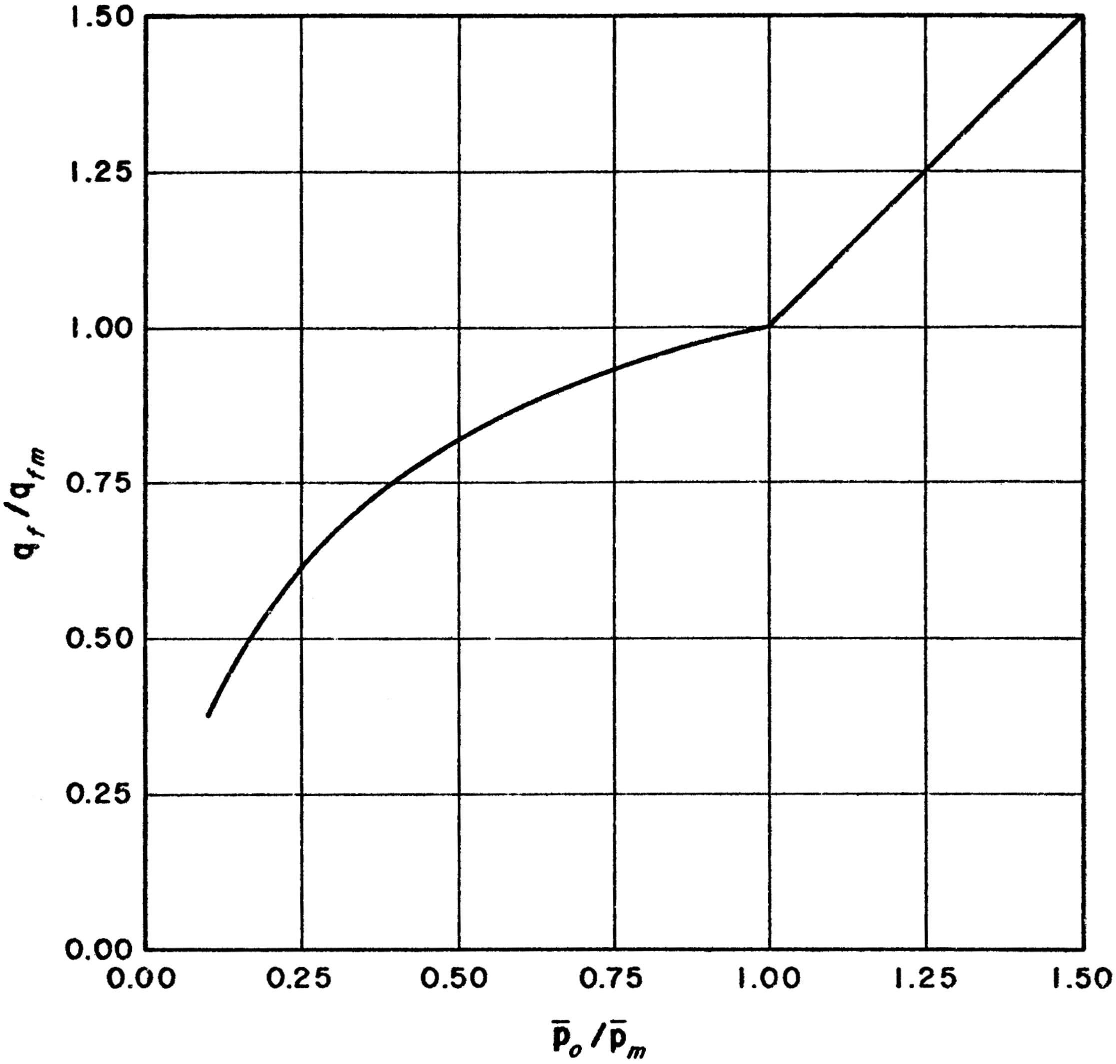

q_f = Shear strength at present effective stress.
q_{fm} = Shear strength at maximum past effective stress.
$\bar{p}_o$ = Present effective stress.
$\bar{p}_m$ = Maximum past effective stress.

Figure 2. Relationship of Undrained Shear Strength to Overconsolidation Ratio.

overconsolidation ratio of two maintained 83 percent of the undrained shear strength it possessed at the maximum consolidation stress.

These authors do not directly address the question of how much the shear strength increases as a result of the overconsolidation. However, a graph is presented from which the shear strength can be estimated if the plasticity index and consolidation stress are known. An example was presented where the shear strength for a soil corresponding to the maximum consolidation stress was computed and then used to predict the shear strength of the same soil at various overconsolidation ratios by utilizing the graph shown in Figure 2.

From the relationships presented by these authors, the increase in shear strength resulting from overconsolidation can be computed. The graph illustrating the variation in the undrained shear strength as a function of plasticity index and consolidation pressure indicates that the shear strength for a particular soil is directly proportional to consolidating stress. Therefore, if the consolidation stress is doubled, the corresponding undrained shear strength is doubled. If the consolidation stress is then reduced to its original value, the soil will have an overconsolidation ratio of two and the strength will be reduced from its maximum value by 17 percent. Thus, the effect of overconsolidating a soil to twice its normally consolidated value is to increase its undrained shear strength by 66 percent. Table I illustrates the increases in shear strength for various overconsolidation ratios used, based on the discussion previously presented.

The authors point out that these relations are useful only in making preliminary estimates of undrained shear strength. It should be noted

TABLE I

INCREASE IN SHEAR STRENGTH RESULTING FROM OVERCONSOLIDATION

Overconsolidation Ratio	Increase in Shear Strength
1.33	25%
1.5	30%
2.0	66%
3.0	98%
4.0	148%

that the overconsolidation ratio for a desiccated soil generally will not be known, thus the use of these relationships to estimate the shear strength of a soil will be limited. However, these relationships do illustrate the fact that even a small amount of overconsolidation could significantly increase the shear strength of a soil.

Parry and Nadarajah (5) examined the effects of small overconsolidations by preparing samples of Kaolin from a slurry and testing them in an undrained condition. The samples were consolidated both isotropically and anisotropically and then tested in triaxial compression and extension. The anisotropic samples were consolidated under a zero lateral strain condition which is commonly referred to as K_0 consolidation.

The test results indicated that the effective stress path for an overconsolidated soil tested in compression was essentially vertical, unless the stress path corresponding to a normally consolidated condition was reached. At low confining pressures, the stress path remained vertical until a failure condition was reached. At high confining pressures, the stress path reached the stress path corresponding to a normally consolidated condition, after which they remained essentially parallel. A marked increase in pore pressure was noted when the two stress paths were in close proximity.

The occurrence of a vertical stress path implied that the average effective stress remained constant as the deviator stress increased. However, when the stress path for the overconsolidated soil reached the stress path corresponding to a normally consolidated soil, the average effective stress decreased rapidly while the deviator stress increased.

This effect can be explained using plastic theory in soils. The deformation is considered elastic only while the stress path is vertical. Therefore, plastic deformation was occurring only over a portion of the loading sequence.

The manner in which the soil was consolidated, whether isotropic or anisotropic, was shown to have an effect on the resulting shear strength. The value determined for the angle of internal friction was 1.8 degrees smaller for the anisotropicly consolidated samples.

It was noted that the increase in deviator stress during the test of the anisotropic normally consolidated sample was small. This fact indicates that a soil which is normally consolidated under K_o conditions has a high degree of instability. However, if the soil is lightly overconsolidated, this instability is eliminated.

These authors point out that surprisingly little work has been conducted on lightly overconsolidated soils. Most of the research has been concentrated on either normally consolidated or heavily overconsolidated soils. They also pointed out that most relatively soft clays are usually lightly overconsolidated. Therefore, the need for additional research to determine the effects of light overconsolidation is apparent.

CHAPTER III

DESCRIPTION OF EMBANKMENT AND FOUNDATION

Introduction

A portion of the research conducted during this study involved an analysis and design of an embankment constructed as part of an interchange on Interstate Highway 70 and U.S. Highway 75 bypass in Topeka, Kansas. This chapter describes the embankment, field investigations, soil properties, and instrumentation used prior, during, and after construction of the embankment.

Embankment

The embankment designed during this study serves as the bridge approach embankment for the upper bridge of a three tier interchange. An overall view of the embankment is presented in Figure 3.

The embankment is approximately 1150 feet long and contains approximately 120,000 cubic yards of compacted soil. The embankment height ranges from zero to approximately forty feet. The embankment was constructed with side slopes of four feet horizontal to one foot vertical except at the high end of the embankment near the bridge approach where the slope was increased to two feet horizontal to one foot vertical. A view of this steepest portion of the embankment is presented in Figure 4. A conceptual view of a portion of the embankment is also presented in Figure 5. It can be seen that there is a cut along the toe of the

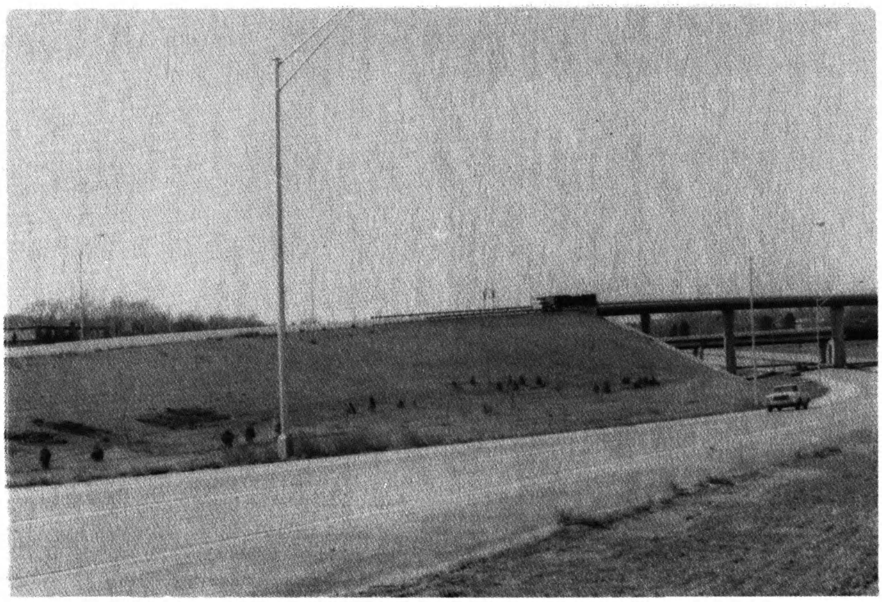

Figure 3. Embankment Constructed as Part of Interstate Highway 70 and U.S. Highway 75 Bypass Interchange

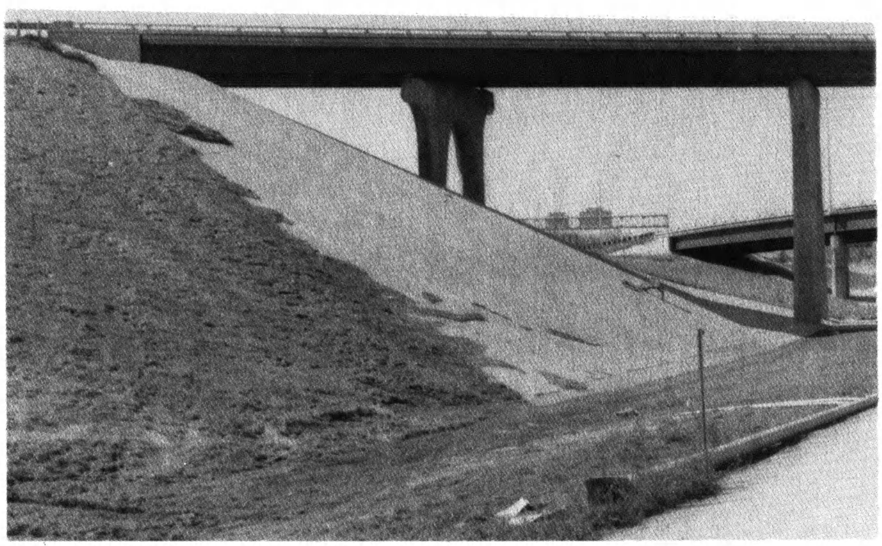

Figure 4. Steepest Portion of the Completed Embankment

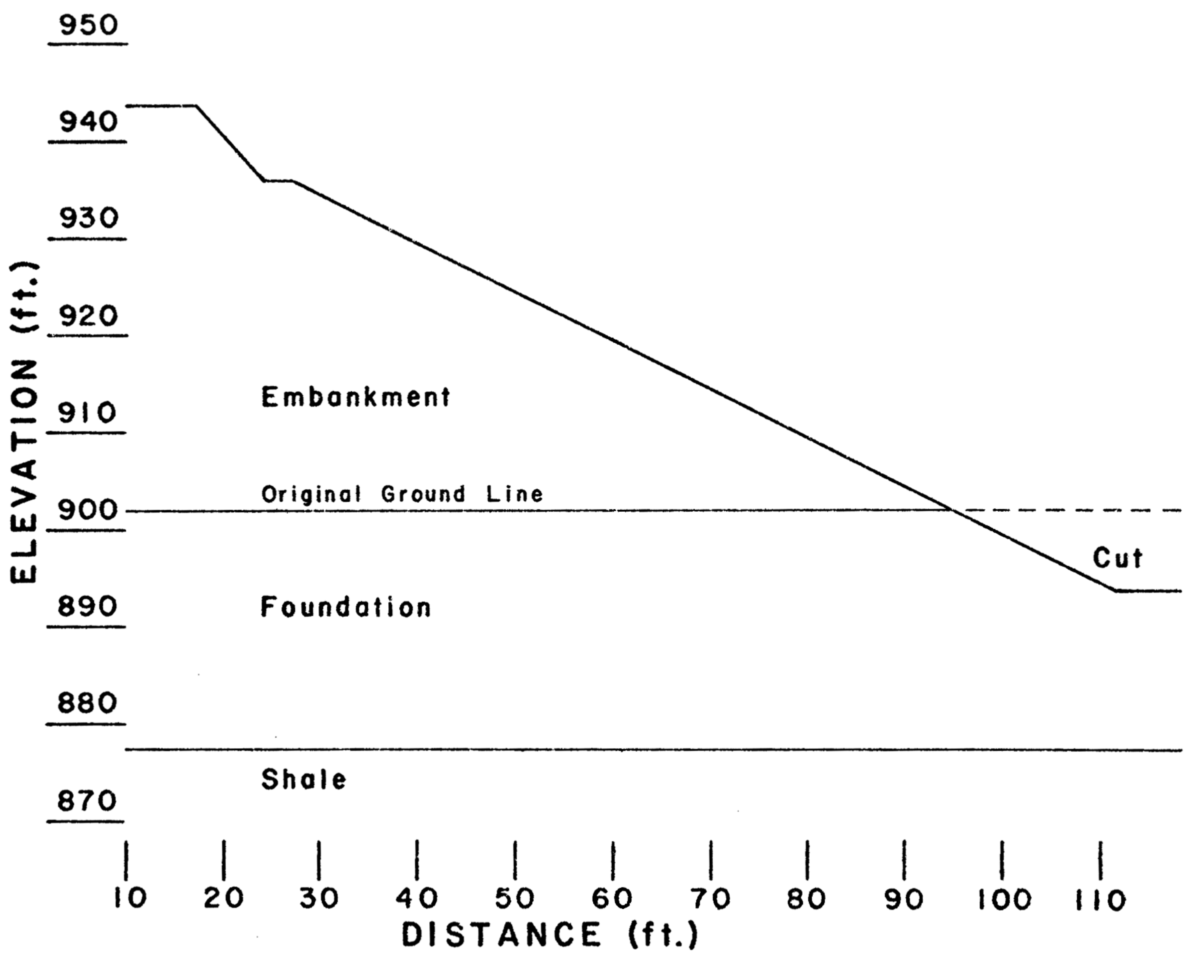

Figure 5. Conceptual View of the Steepest Portion of the Embankment.

embankment at this location which extends the slope to an effective overall height of approximately fifty feet.

The embankment was constructed according to the specifications developed by the Kansas Department of Transportation (KDOT) for type B compaction and MR-5 moisture control. The specifications required that compaction continue until the roller walked out of the compacted soil and rode on the top of the lift. The water content during compaction was maintained at a minimum of 95 percent of the standard Proctor optimum water content as determined by ASTM D-698. Construction of the embankment was completed in 1976 with the major portion constructed during a two week period in July. It should be noted that, because of the special instrumentation which was used, the embankment was carefully monitored during construction to ensure that the design specifications were met.

The steepest portion of the embankment slope and the portion of the slope directly under the bridge were covered with four inch concrete riprap. This riprap can be seen in Figure 4. The riprap is used for erosion control and esthetics and has no meaningful effect on the embankment stability.

The compacted embankment soils came from excavations made in the vicinity and are therefore similar to the foundation soils described subsequently. The grain size characteristics of the embankment soils have been summarized and are presented in Table II. The physical properties of the embankment soils are summarized in Table III. The standard compaction tests on the embankment soil yielded a standard proctor density of 100 pounds per cubic foot dry weight and an optimum water content of 21.5%. All tests were conducted according to KDOT standard test procedures.

TABLE II - EMBANKMENT SOIL GRAIN SIZE

Sample Number	Percent Passing								
	Sieve Analysis				Hydrometer Analysis				
	Standard Sieve Size				Particle Size (Millimeters)				
	10	40	100	200	.05	.03	.01	.005	.002
A-1	100	100	99	97	89	71	37	28	22
B-1	100	99	96	91	86	75	47	37	30

TABLE III - PHYSICAL PROPERTIES OF EMBANKMENT SOILS

Sample Number	Liquid Limit	Plastic Limit	Plasticity Index	Specific Gravity	Classification
A-1	36	22	14	2.63	CL
B-1	42	22	20	2.65	CL

Foundation

The foundation soils at this location were identified as being basically fluvial in origin. Fluvial soils generally consist of sand and silt and may contain clay. Fluvial soils generally become coarser with depth.

The first step in the subsurface investigation prior to construction of the embankment was to review any available information on conditions and characteristics of the soil in the area of the proposed embankment and utilize this information to plan the field investigation. The information available to KDOT included a Soil Survey conducted for the construction of Interstate 70 and the logs of borings made for the design of the footings to be used on the proposed bridge. In addition, a Soil Survey conducted for Shawnee County by the Soil Conservation Service was reviewed.

All of the available information indicated that the subsoils were uniform throughout this area and were underlain by a virtually level shale formation at an average depth of 25 feet. Because of the wealth of information available within the immediate area of the embankment, it was believed that only one additional boring would be required. This boring was taken near the toe of the proposed embankment.

The first phase of the subsurface investigation consisted of logging the soils. This logging was accomplished by using a Bull Soil Sampler (BSS). The BSS is used to hydraulically push the sample tube into the ground to obtain a soil sample. The sample tube consists of a 1 1/8 inch diameter tube which has a portion of one side cut away so that the soil can be viewed while still in the tube. These samples formed the basis of the boring log which is in Appendix A.

The second phase of the subsurface investigation consisted of taking several undisturbed samples. Based on the information obtained in the first phase of the investigation, the soil profile consisted of approximately one foot of topsoil, sixteen feet of uniform silty clay, and seven feet of clay loam over shale. The topsoil was to be removed before construction of the embankment so it was not sampled. One set of samples were taken from each of the two remaining soil layers. Each set consisted of three samples.

The undisturbed samples were taken using a three inch diameter seamless steel thin walled Shelby tube. Continuous flight hollow stem augers were used for drilling to the required depths. The sample was obtained by lowering the sampler through the hollow auger at the desired depths.

After construction of the embankment, thirty additional undisturbed samples of the foundation soils were taken using a three inch diameter Shelby tube sampler. This sampling was conducted at a location near the embankment, but not within the area of influence of the embankment. Twenty-one of these samples were taken at a depth of five feet, two at a depth of ten feet, three at a depth of fifteen feet, and four at a depth of twenty feet.

The laboratory analysis of these soils showed that they contain fine sand, silt, and clay with silt being the most predominant particle size. The soils classify as inorganic clay of low to medium plasticity (CL) according to the Unified Classification system.

The grain size characteristics of the foundation soils are summarized in Table IV. The physical properties of the foundation soils are summarized in Table V.

A total of twenty-four samples were taken from 1.2 feet to 17.6 feet in depth. Two reports of soil tests summarizing these twenty-four samples are included in Appendix A. The first shows the limits within which all of the tests fell. The second shows the averages of the tests from various depths within the strata. There is a slight increase in the quantity of fine sand and a corresponding decrease in the quantity of silt as depth increases. This increase in sand is typical of fluvial deposits. The variation in grain size is small and would not indicate any significant change in the soil strength.

Comparing the liquid limit (LL), plastic limit (PL) and plasticity index (PI) for the twenty-four samples from this strata, as shown in Table V, it can be seen that the PL remains relatively constant throughout the strata. However, there is a slight decrease in the LL which results in a decrease in the PI with depth. The average LL of the sixteen samples from a depth of approximately five feet is 39.0. This average dropped to 38.6 for the five samples from a depth of approximately ten feet and 35.3 for the three samples from a depth of approximately fifteen feet.

A statistical analysis was performed to determine whether the tests indicated a significant change in the LL or whether this variation could be accounted for a sampling variation. At a level of significance of 0.01, this analysis indicated that the LL variation cannot be considered to be significant when comparing samples from a depth of five feet with those from a depth of ten feet or when comparing samples from a depth of ten

TABLE IV - Foundation Soil Grain Size

Sample Number	Depth	Percent Passing								
		Sieve Analysis Standard Sieve Sizes				Hydrometer Analysis Particle Size (Millimeters)				
		10	40	100	200	.05	.03	.01	.005	.002
1-1	5.8	100	99	96	93	87	73	37	26	20
2-1	4.5	100	100	98	94	87	72	38	28	18
3-1	4.7	100	100	98	94	87	72	41	30	20
4-1	4.7	100	100	99	95	88	74	38	29	22
5-1a	4.5	100	100	99	95	88	75	42	30	24
5-1b	5.1	100	100	99	95	88	73	37	28	21
6-1	4.9	100	100	99	95	87	70	41	32	24
7-1	4.5	100	100	99	97	91	76	39	29	22
8-1	4.6	100	100	99	96	89	74	40	32	25
13-1	4.7	100	100	98	94	88	73	38	28	22
14-1	4.6	100	99	97	94	85	72	36	26	20
15-1	4.5	100	100	99	96	90	76	41	30	24
16-1a	4.4	100	100	99	96	90	77	43	32	24
16-1b	5.1	100	100	98	94	88	73	39	30	24
17-1	4.6	100	100	98	95	88	74	36	28	22
18-1	4.7	100	100	98	95	88	74	40	30	24
18-2	9.6	100	97	90	82	76	64	40	30	23
18-3	11.0	100	97	90	82	76	68	43	34	28
1T	10.4	100	100	99	97	90	77	45	31	22
2T	11.0	100	99	98	95	90	80	42	30	20
3T	12.0	100	99	98	95	90	80	42	30	20
17-3	15.6	100	99	92	84	76	65	40	30	23
18-4	14.5	100	99	92	85	77	64	39	29	22
18-5	16.3	100	99	95	88	82	69	42	31	24
17-4	20.6	100	99	89	79	71	60	36	26	16
18-6a	19.3	100	100	92	82	75	63	37	27	18
18-6b	19.9	100	99	91	81	72	60	35	25	14
18-7	21.4	98	83	73	64	58	50	35	26	18
1C-3A	19.3	100	99	93	82	73	62	39	30	23
1C-3B	21.0	100	99	92	82	73	61	38	29	22
1C-3C	22.5	100	96	86	74	66	56	36	27	20

TABLE V - Physical Properties of Foundation Soils

Sample Number	Liquid Limit	Plastic Limit	Plasticity Index	Specific Gravity	Classification
1-1	37	21	16	2.60	CL
2-1	38	20	18	2.63	CL
3-1	39	21	18	2.65	CL
4-1	39	21	18	2.63	CL
5-1a	40	21	19	2.63	CL
5-1b	39	20	19	2.65	CL
6-1	40	20	20	2.63	CL
7-1	40	20	20	2.65	CL
8-1	39	20	19	2.63	CL
13-1	37	20	17	2.60	CL
14-1	39	20	19	2.72	CL
15-1	39	20	19	2.65	CL
16-1a	40	20	20	2.63	CL
16-1b	38	21	17	2.62	CL
17-1	40	22	18	2.60	CL
18-1	40	21	19	2.63	CL
18-2	42	20	22	2.67	CL
18-3	37	19	18	2.67	CL
1T	39	19	20	2.67	CL
2T	39	20	19	2.65	CL
3T	36	21	15	2.65	CL
17-3	36	20	16	2.63	CL
18-4	36	21	15	2.65	CL
18-5	34	20	14	2.65	CL
17-4	31	19	12	2.65	CL
18-6a	33	20	13	2.63	CL
18-6b	32	20	12	2.62	CL
18-7	32	20	12	2.70	CL
1C-3A	34	18	16	2.62	CL
1C-3B	36	20	16	2.62	CL
1C-3C	35	20	15	2.65	CL

feet with those from a depth of fifteen feet. However, the change in LL is significant if the samples from a depth of five feet are compared with those from a depth of fifteen feet. Although this analysis does indicate that the LL and PI do decrease with depth, the change is very slight and would not indicate any significant change in strength with depth.

Instrumentation

The instrumentation used during the construction of the embankment consisted of piezometers to measure pore water pressure and an inclinometer to measure any movement of the foundation soil. The locations of the instrumentation are shown in Figure 6.

The piezometers were the pneumatic pressure type which were manufactured by the Slope Indicator Company. The piezometer tips were surrounded by sand and placed at the points shown in Figure 6. The drill hole was sealed using commercial bentonite pellets. The tips were made from a porous material with diaphragms and tubes for containing the nitrogen gas used in the portable readout. The support equipment consisted of a gas supply, metering device, and various gauges. When a reading was taken, gas from the readout device passed to the tip where it opened the diaphragm and was vented to the atmosphere. The gas flow was then stopped and the pressure dropped until the diaphragm closed causing the escape of gas to stop. At this point, the gas pressure on one side of the diaphragm was equal to the water pressure on the other side of the diaphragm, so measurement of the gas pressure gave the measurement of the pore pressure directly.

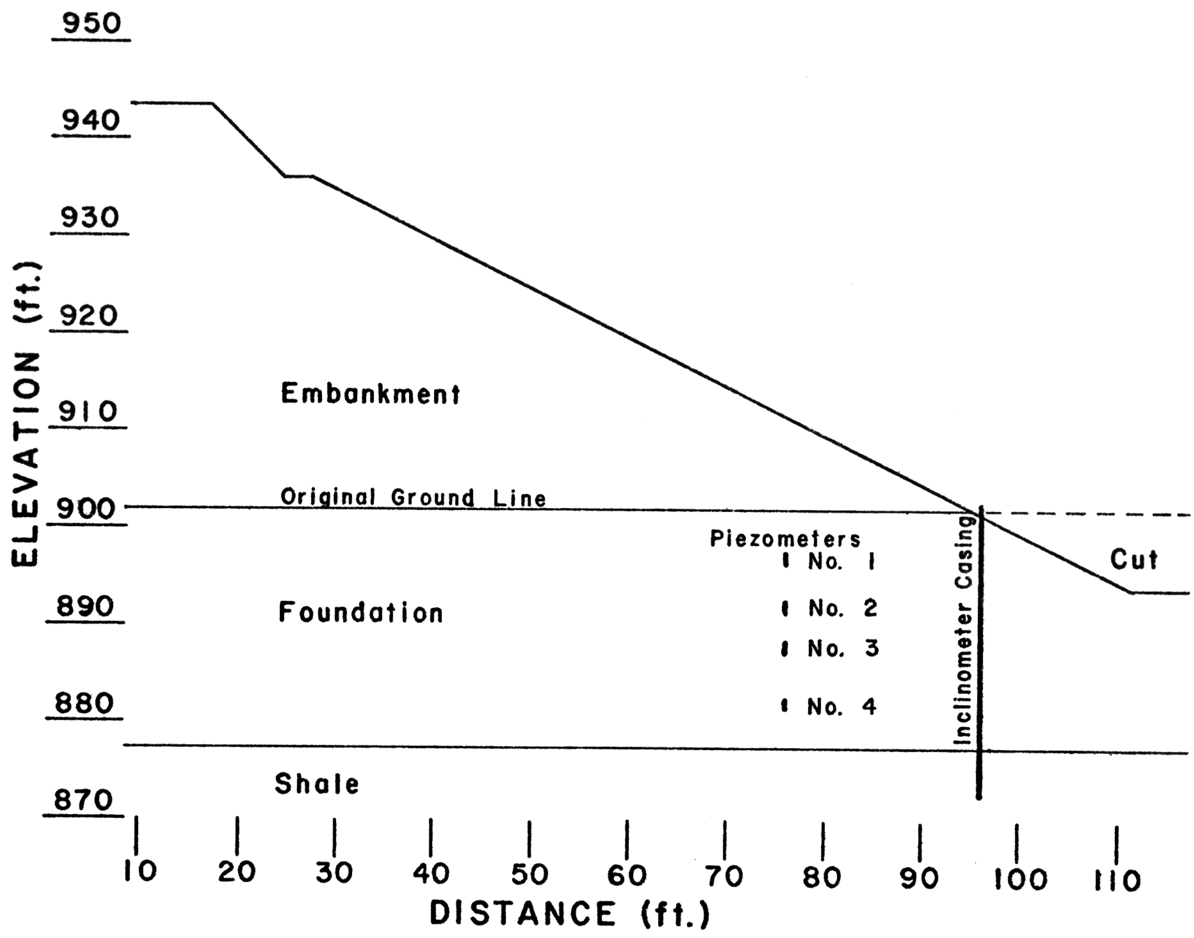

Figure 6. Conceptual View of the Embankment Showing the Location of the Instrumentation.

The inclinometer was also manufactured by the Slope Indicator Company. The inclinometer consisted of a probe which is lowered into a grooved aluminum casing, and a readout device which is connected to the probe by wires. The probe consisted of a pendulum and variable resistor which serves as part of a Wheatstone Bridge. The readout device made up the remainder of the Wheatstone Bridge.

The probe was lowered down the casing and the inclination of the casing was correspondingly determined at various intervals. The inclination was used to compute the embankment deflections. In this way, any movement in the soil which would result in the movement of the casing was measured.

CHAPTER IV

TEST RESULTS

The results of the triaxial tests are presented in the first section of this chapter. The pore pressure and deformations measured by the field instrumentation are presented in the last section.

Triaxial Test Results

The test results are presented in three groups: foundation samples taken before construction, embankment samples taken during construction, and foundation samples taken after construction. The last group is further divided into samples tested by the Kansas Department of Transportation and those tested by the University of California at Berkeley.

Foundation Samples Taken Before Construction

This group consists of two sets of samples with three samples per set. The locations where the samples were taken are shown on the boring log presented in Appendix A.

The triaxial test results are shown in Figures 7 and 8. A summary of the test results is presented in Table VI. Samples 1-T, 2-T, and 3-T were tested by a modified test procedure consisting of the following steps: saturation on the vacuum saturator, consolidation to the confining stress with free drainage and then loaded in the undrained condition. Samples 1C-3A, 1C-3B, and 1C-3C were tested according to standard

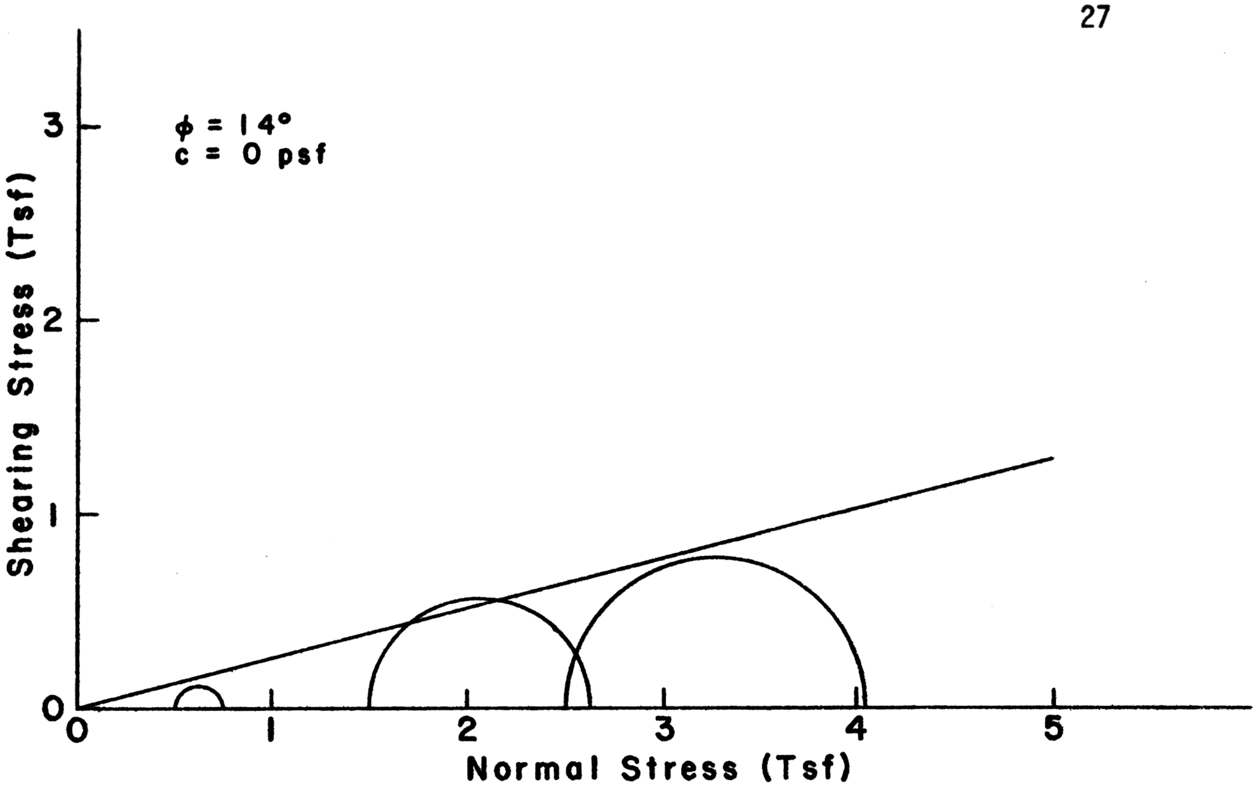

Figure 7. Triaxial Test Results, Samples 1T, 2T, 3T

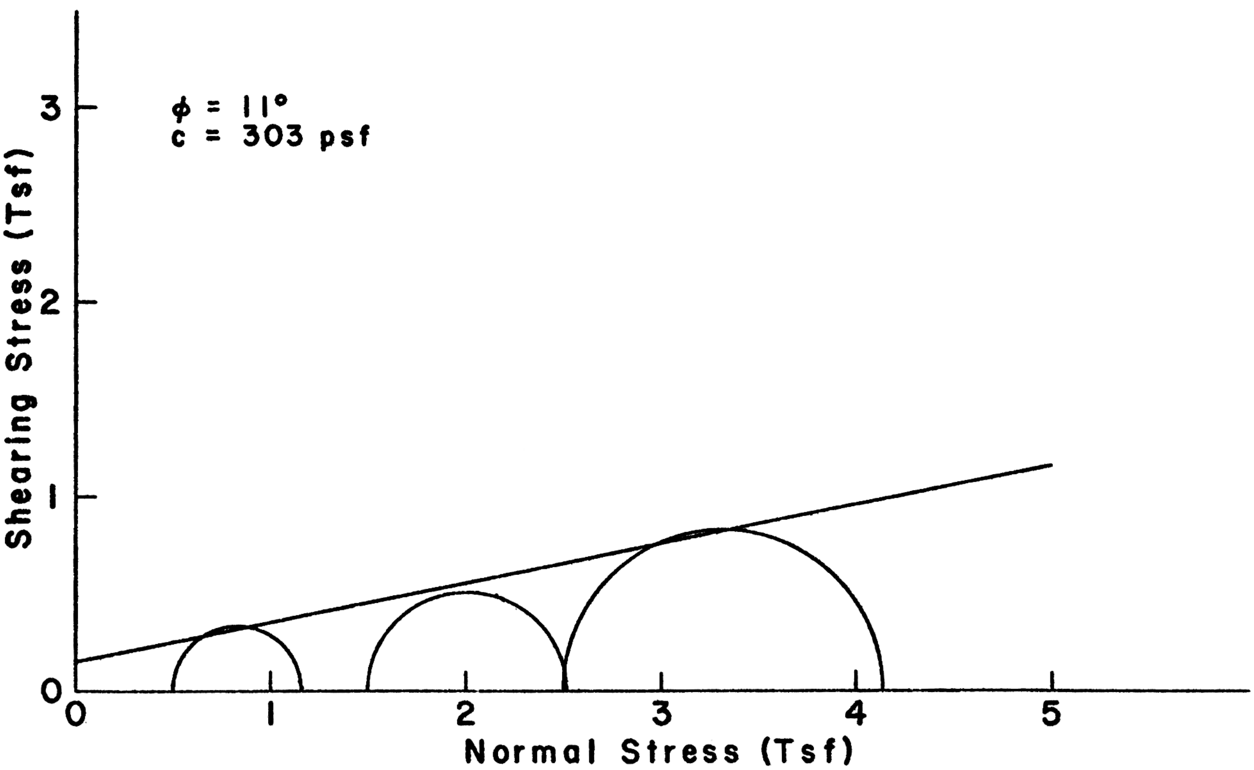

Figure 8. Triaxial Test Results, Samples 1C-3A, 1C-3B, 1C-3C

TABLE VI - TRIAXIAL TEST RESULTS, FOUNDATION SOILS

Sample Numbers	Depth (Ft.)	Chamber Pressure Range (TSF)	c	ϕ	c'	ϕ'
1T, 2T, 3T	10.1-12.4	0.5-2.5	0	14	180	22.5
1C-3A, 1C-3B 1C-3C	19.0-22.9	0.5-2.5	303	11	332	19.4

TABLE VII - TRIAXIAL TEST RESULTS, EMBANKMENT SOILS

Sample Numbers	Location	Chamber Pressure Range (TSF)	c	ϕ
A-1, A-2, A-3	Elev. 910.5	0.5-2.5	3,338	15
B-1, B-2, B-3	Elev. 919	0.5-2.5	1.048	6

Kansas Department of Transportation test procedures. These procedures include saturating the samples on the vacuum saturator, using backpressure saturation, and testing the samples in the consolidated undrained condition with pore pressure measurements.

Embankment Samples Taken During Construction

The group consisted of two sets of samples with three samples per set. The samples were taken from the embankment at two different elevations as the embankment was constructed.

The results of the triaxial tests conducted on these samples are presented in Figures 9 and 10. A summary of the test results is also presented in Table VII. These tests were conducted using the in-situ water content under the unconsolidated undrained condition with pore pressure measurement taken. The strain rate was adjusted to provide a constant rate of strain of two percent per hour.

Foundation Samples Taken After Construction

After construction of the embankment, thirty additional undisturbed samples were taken from the foundation soils at a location adjacent to the embankment. The thirty samples were tested in nine sets with from two to six samples per set. The results of these tests are presented in Figures 11 through 19. The results are also summarized in Table VIII.

Field Instrumentation Results

The results of the field instrumentation are presented in Figures 20 through 22. Figure 20 presents the pore pressure measurements and the

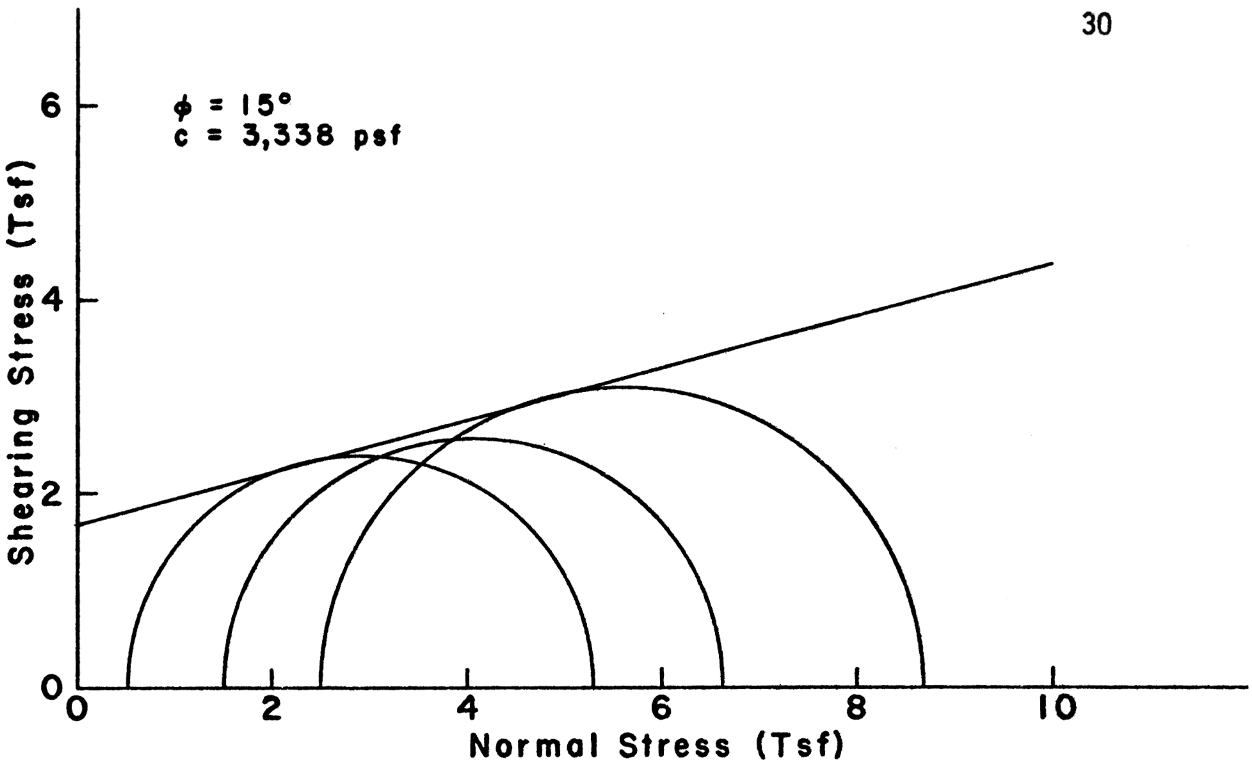

Figure 9. Triaxial Test Results, Samples A-1, A-2, A-3.

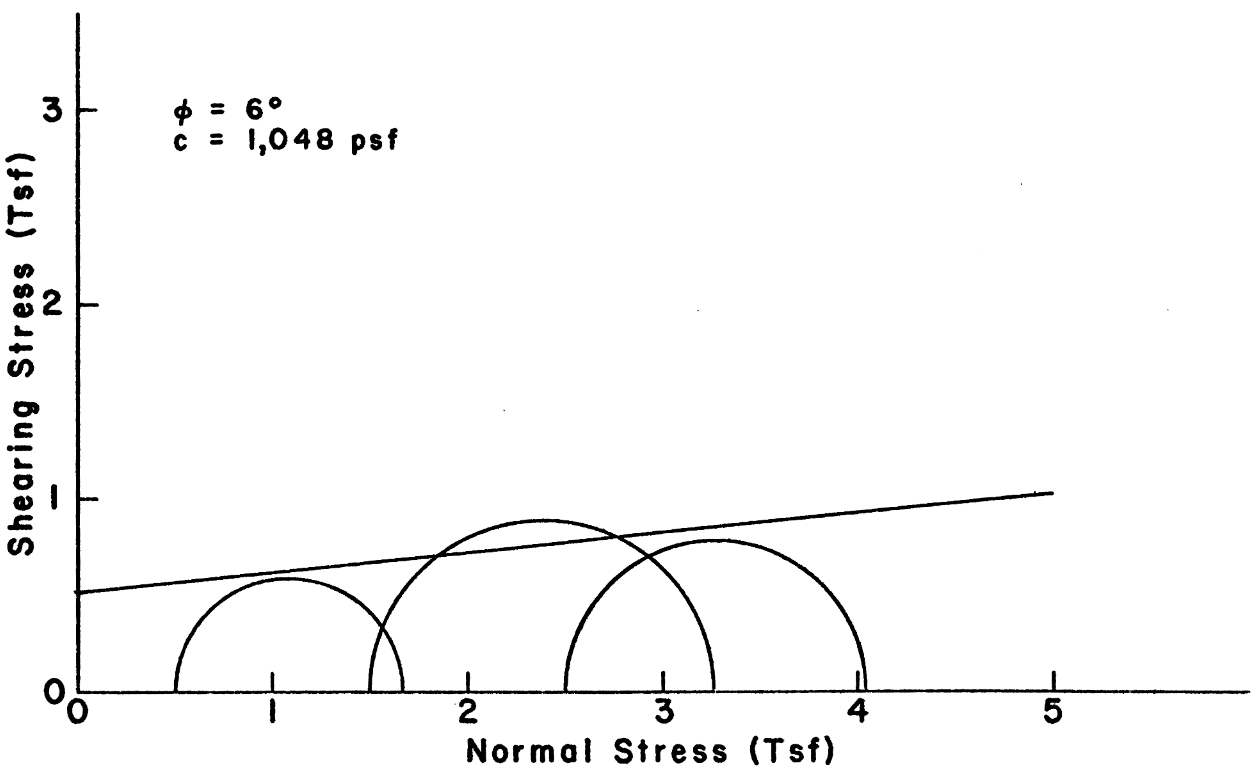

Figure 10. Triaxial Test Results, Samples B-1, B-2, B-3.

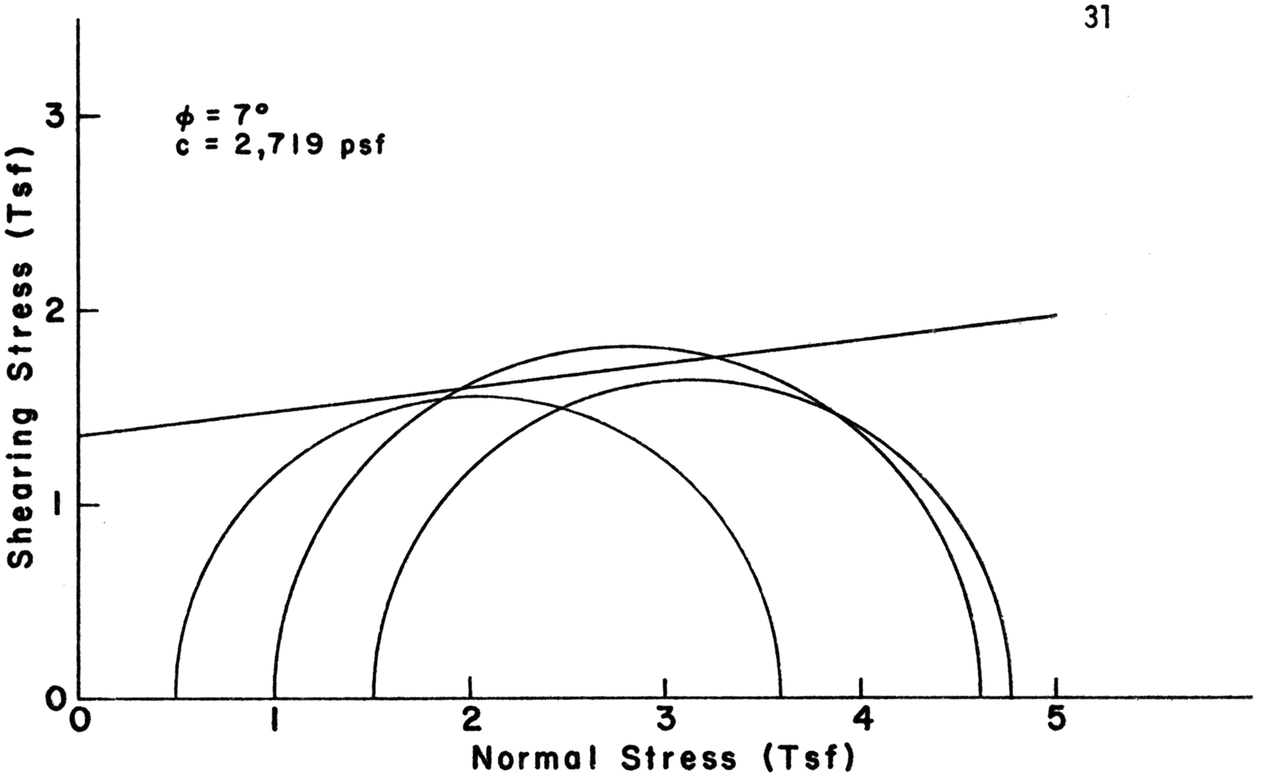

Figure 11. Triaxial Test Results, Samples 14-1, 15-1, 16-1a.

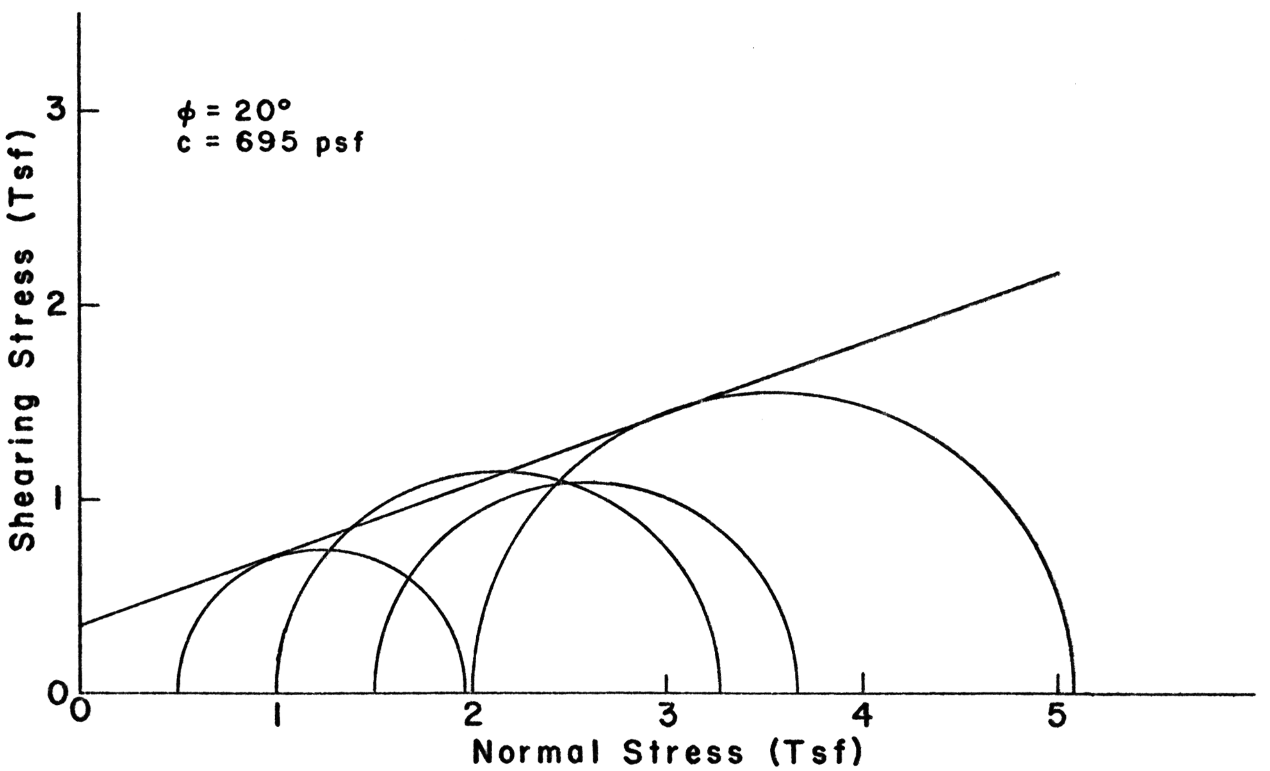

Figure 12. Triaxial Test Results, Samples 17-1, 16-1b, 18-1, 13-1.

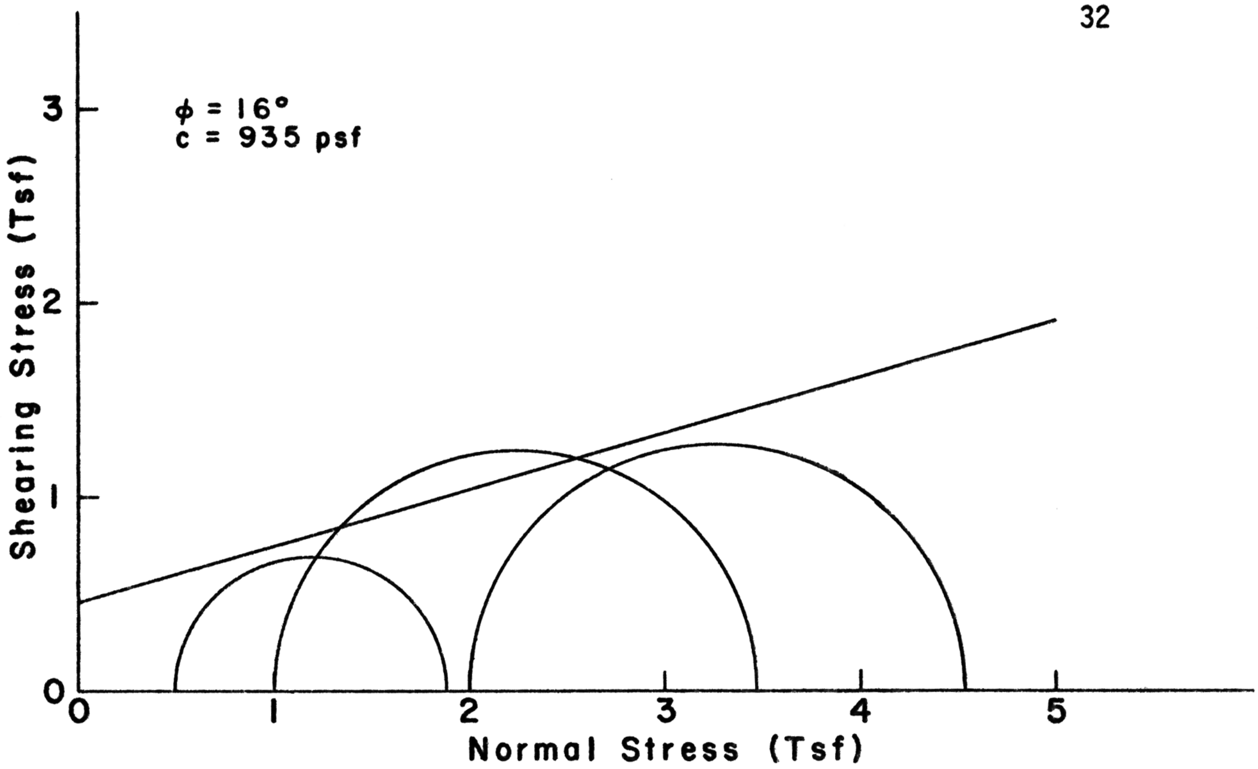

Figure 13. Triaxial Test Results, Samples 1-1, 7-1, 8-1.

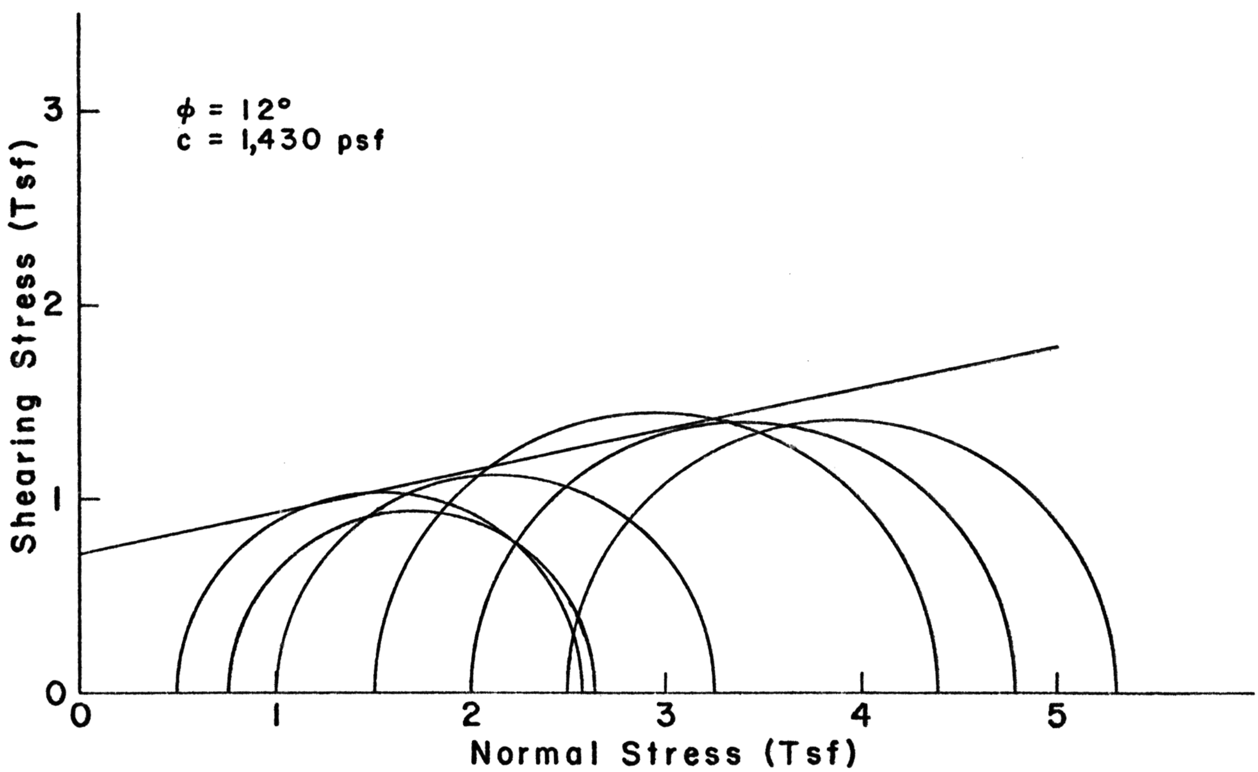

Figure 14. Triaxial Test Results, Samples 2-1, 3-1, 4-1, 5-1a, 5-1b, 6-1.

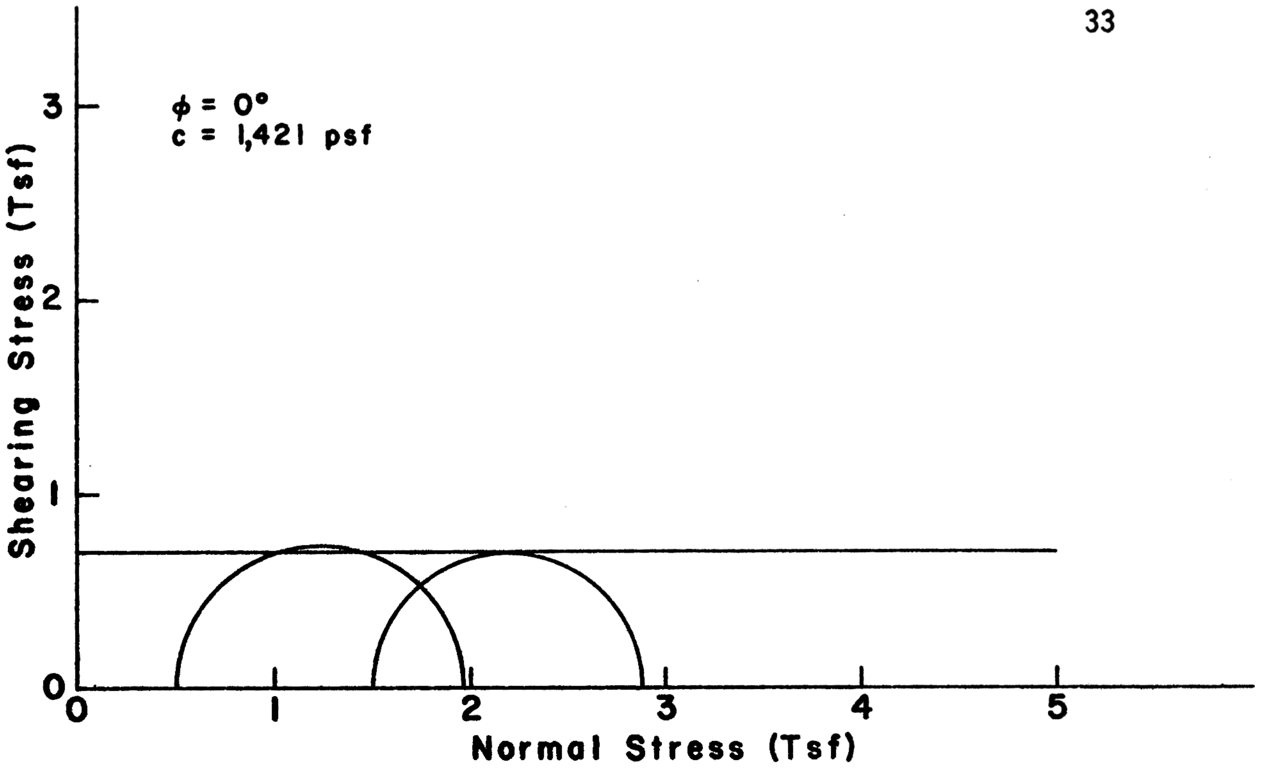

Figure 15. Triaxial Test Results, Samples 18-2, 18-3.

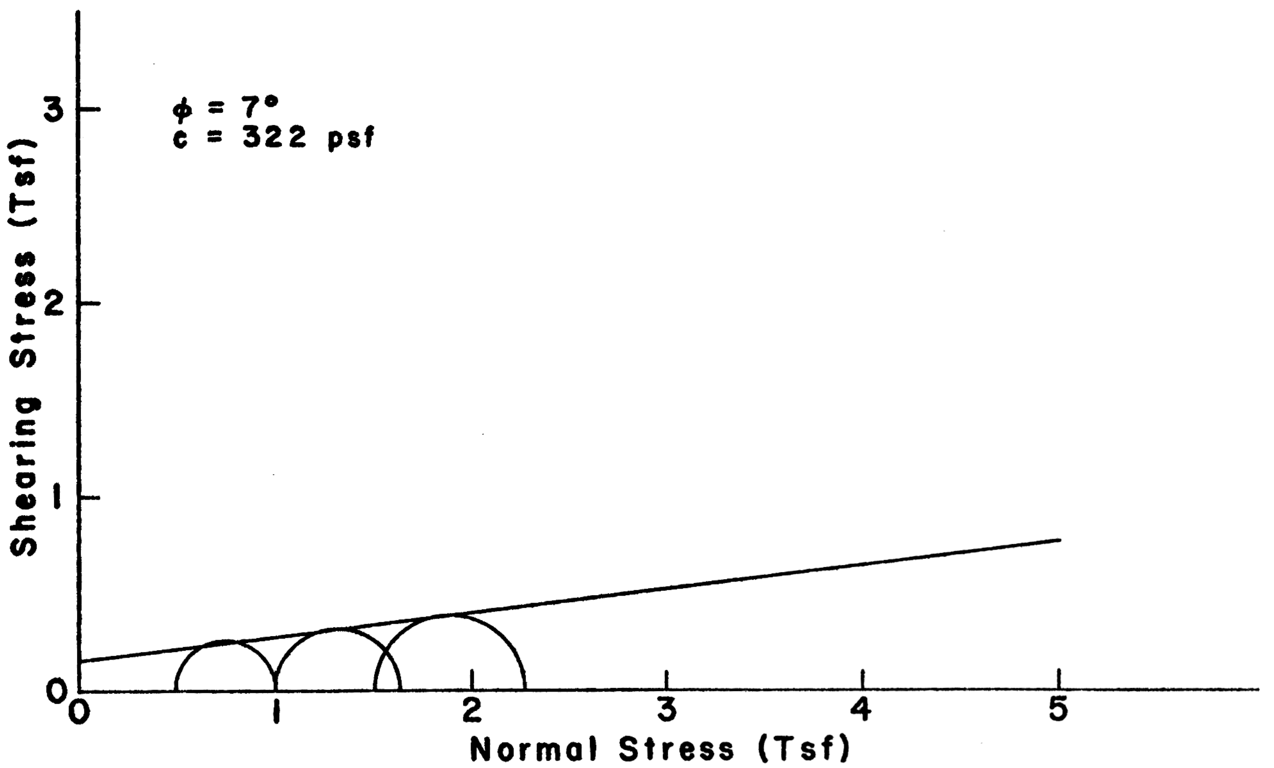

Figure 16. Triaxial Test Results, Samples 17-3, 18-4, 18-5.

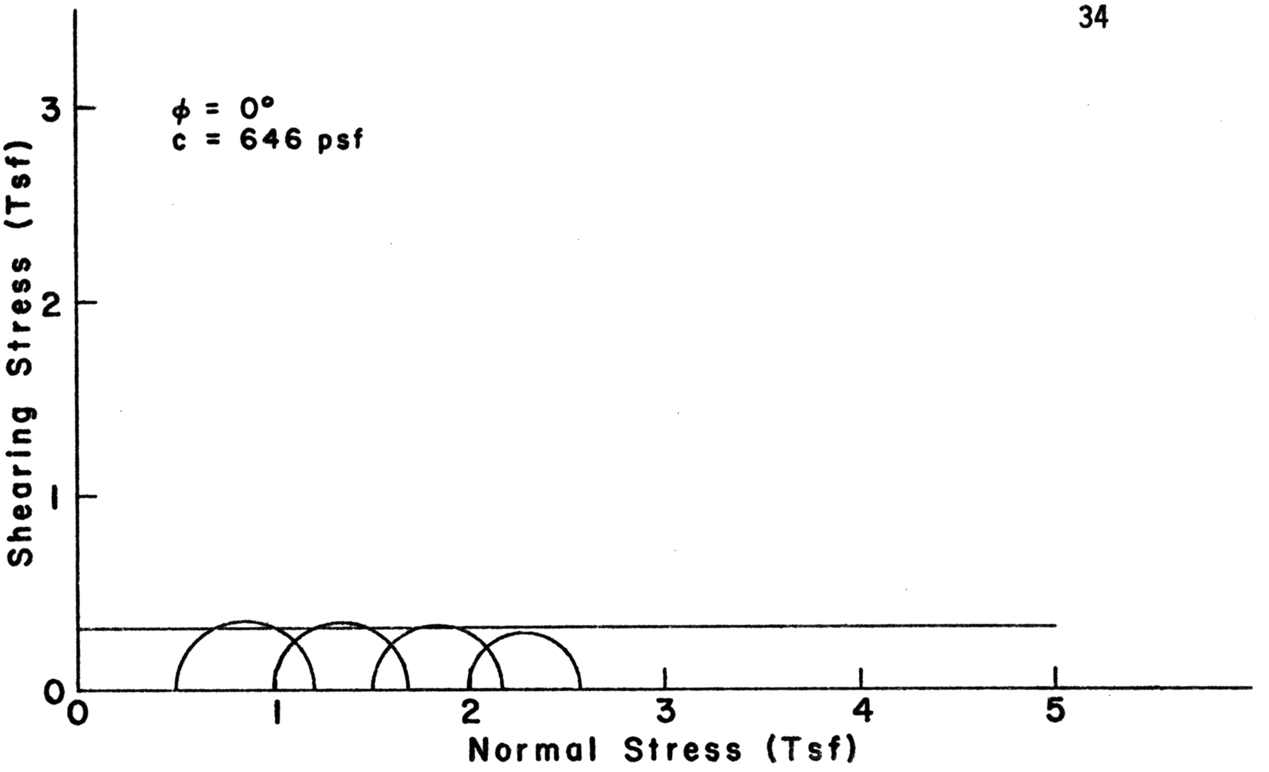

Figure 17. Triaxial Test Results, Samples 18-6a, 18-6b, 18-7, 17-4.

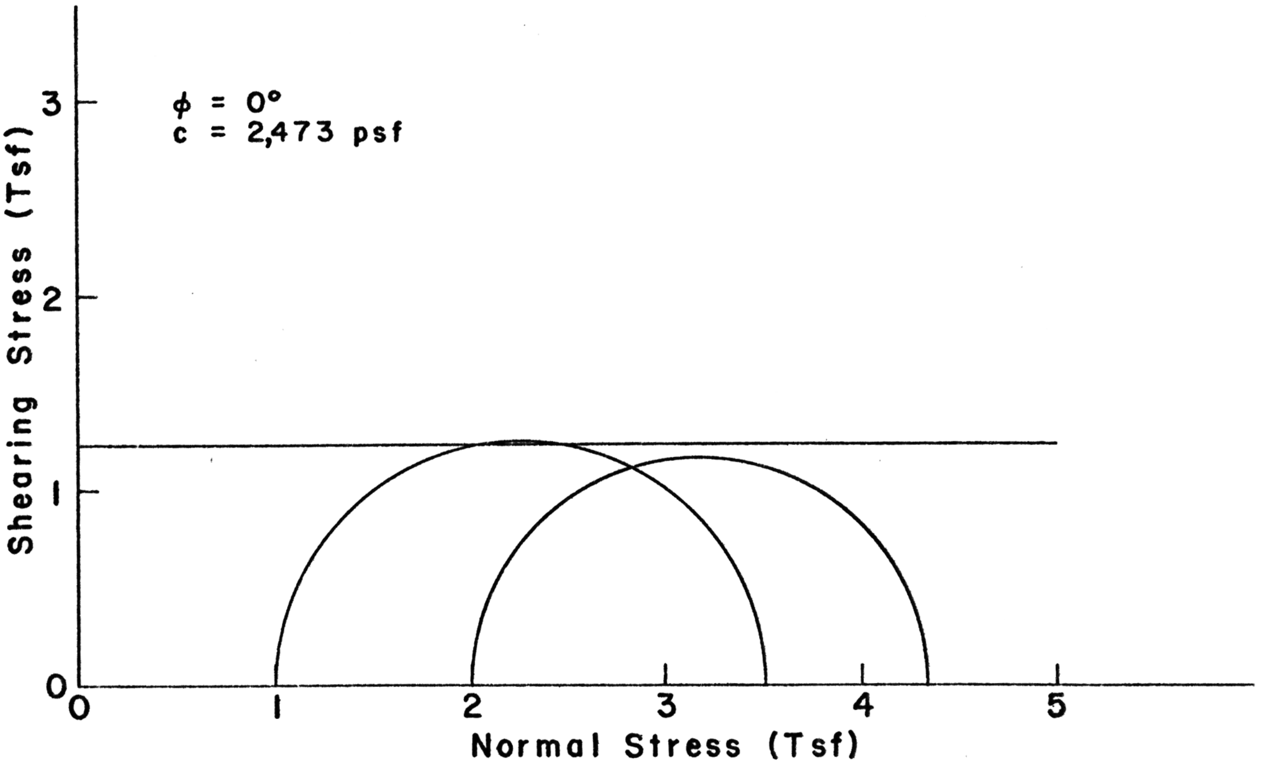

Figure 18. Triaxial Test Results, Samples 9-1-2, 11-1-2.

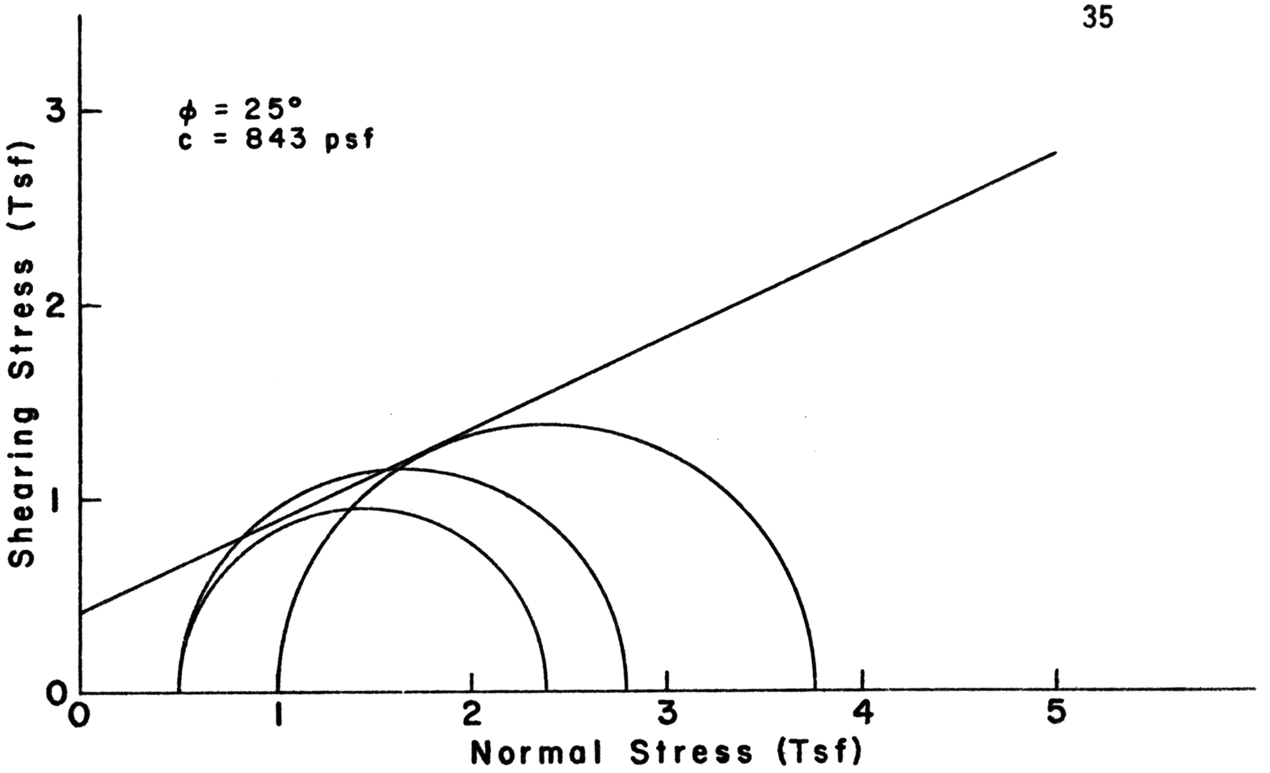

Figure 19. Triaxial Test Results, Samples 12-1-3, 9-1-3, 11-1-1.

TABLE VIII - TEST RESULTS, POST CONSTRUCTION SAMPLES

Sample Numbers	Depth (Ft.)	Type Test	Strain Rate (%/hr.)	Pressure Range (TSF)	c (PSF)	ϕ (degrees)	Remarks
TESTS BY KANSAS DEPARTMENT OF TRANSPORATION							
14-1, 15-1 16-1a	5	CU	2	0.5-1.5	2,719	7	Vacuum Saturation
13-1, 16-1b 17-1, 18-1	5	CU	2	0.5-2.0	695	20	Back Pressure Saturation
1-1, 7-1, 8-1	5	UU	5	0.5-2.0	935	16	As Cut Moisture
2-1, 3-1, 4-1 5-1a, 5-1b 6-1	5	UU	60	0.5-2.5	1,430	12	
18-2, 18-3	10	UU	60	0.5-1.5	1,421	0	
17-3, 18-4	15	UU	60	0.5-1.5	322	7	
17-4, 18-6a 18-6b, 18-7	20	UU	60	0.5-2.0	646	0	
TESTS BY UNIVERSITY OF CALIFORNIA AT BERKELEY							
9-1-2, 11-1-2	5	UV	*	1.02-2.05	2,473	0	
12-1-3, 9-1-3 11-1-1	5	CU	**	0.51-1.02	843	25	

* controlled stress test (strain equaled 20% in 30 minutes or less)
** controlled stress test (strain equaled 20% in 3 hours or less)

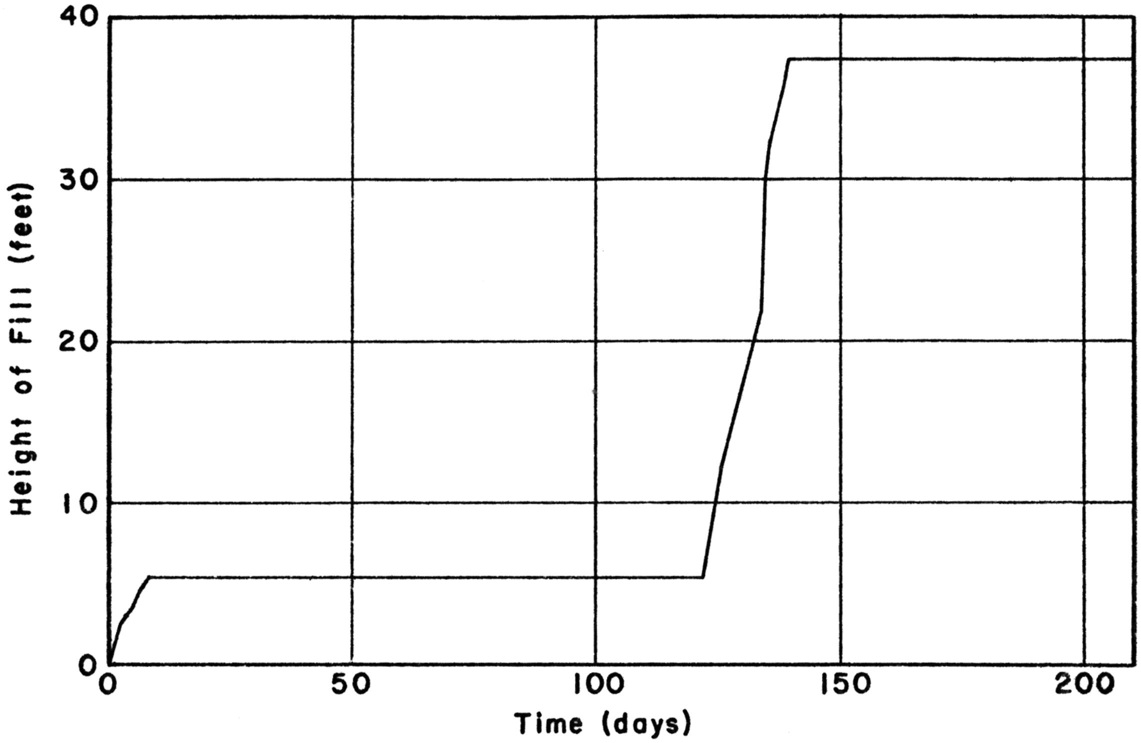

a. Embankment Construction

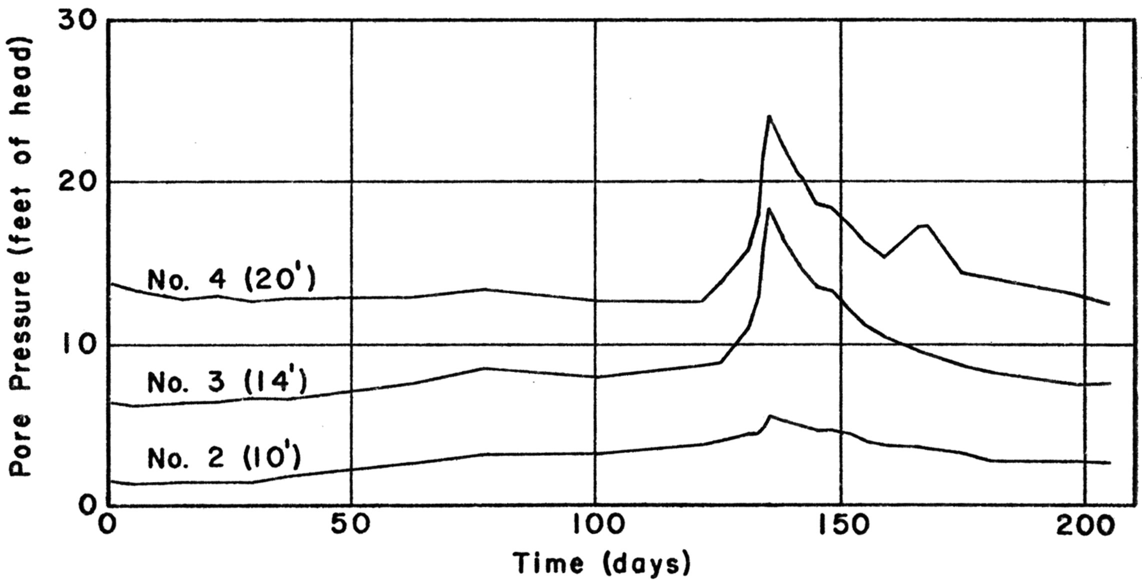

b. Measured Pore Pressure

Figure 20. Pore Pressure Measurements and Embankment Construction as Related to Construction Time.

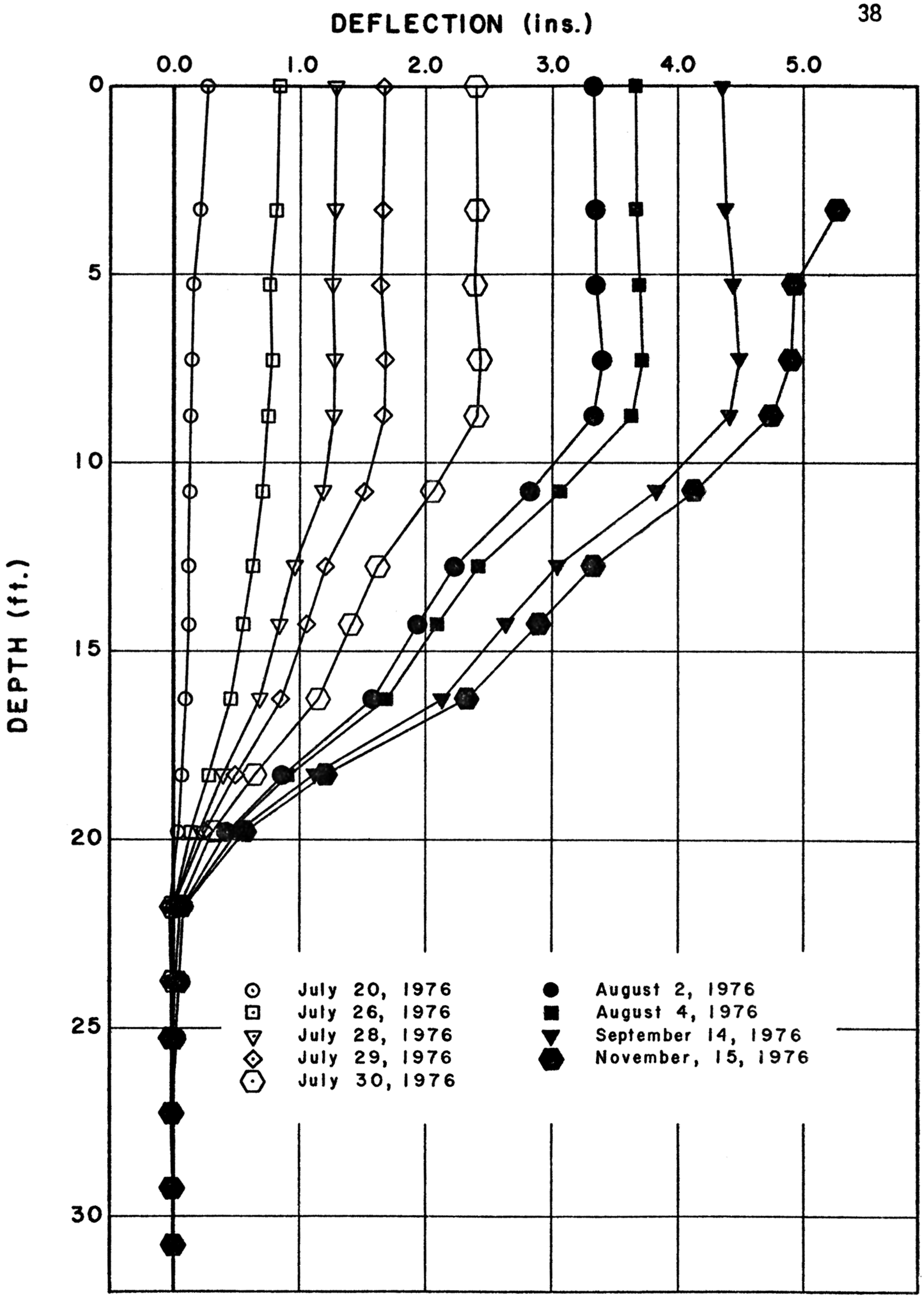

Figure 21. Deflection of Inclinometer Casing.

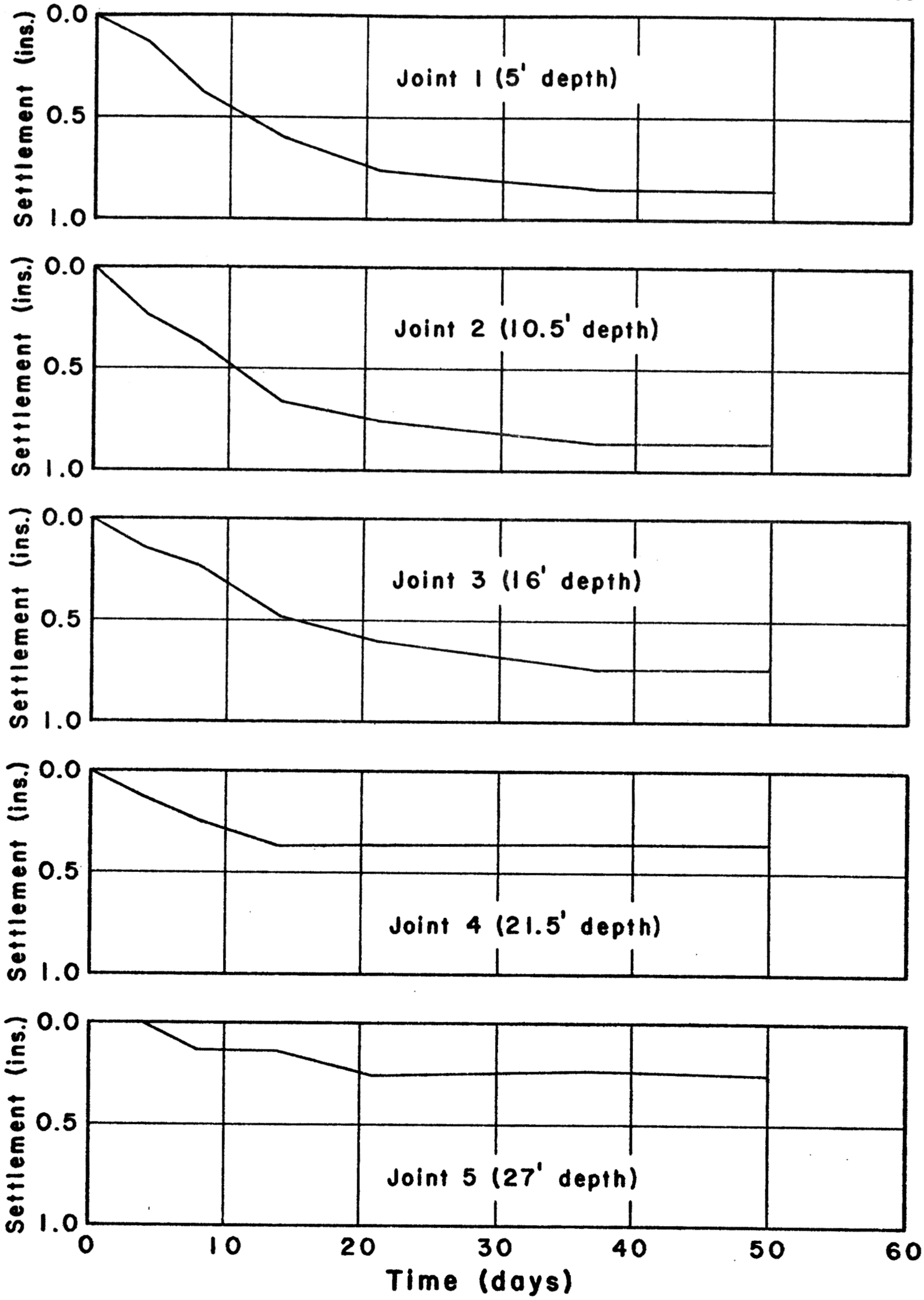

Figure 22. Settlement Measured at the Inclinometer Joints.

embankment height expressed as a function of the construction time. Piezometer number one was located at a depth of five feet. The water level had dropped below the five foot level by the time the piezometer was installed and therefore no significant pore pressure was ever measured at this depth. Piezometers two, three, and four did show an increase in pore pressure within the embankment as construction progressed.

The deformation of the soil was measured by the deflection of the inclinometer casing as described previously. The deflection of the inclinometer casing, expressed as a function of time, is presented in Figure 21. As can be seen in this figure, the top of the inclinometer casing moved horizontally almost four inches as the embankment was constructed. In addition, some movement has taken place since completion of the construction sequence. It can also be seen that approximately the upper ten feet of the casing stayed essentially vertical while the lower portion of the casing underwent major deformation to a depth of approximately twenty-two feet. The deflected shape of the inclinometer casing is of considerable significance to this study since it confirms that the upper soils that had undergone desiccation did not deform although the lower soils did deform considerably.

Figure 22 shows the settlement of the inclinometer casing as measured at its joints. It is important to note that the settlement was less than one inch for any of the joints. Another important point is that the top two joints moved down equal amounts, thus indicating that no consolidation had taken place in the top ten feet. However, each of the remaining joints moved closer together with the greatest relative movement being between joints three and four, thus indicating that the maximum consolidation occurred in the strata between sixteen and twenty-one feet.

CHAPTER V

STABILITY AND DEFORMATION ANALYSIS

Presented in this chapter are the results of two different methods of analysis performed on the embankment. The first method of analysis presented is that of a conventional slope stability procedure utilizing a circular arc form of failure. The second method consists of a slope stability analysis using a method of finite elements. The effect of desiccation on the deformation and stability of the embankment as determined by both methods of analysis is presented and discussed.

Slope Stability Analysis

A simplified form of the method of stability analysis as developed by Bishop (6) was used. In this analysis, a circle representing a possible failure surface was passed through the embankment and the area above the circle was divided into vertical slices. The weight of each slice was computed and resolved into components, with one component acting along the potential failure surface and the other component acting perpendicular to the potential failure surface. The weight component which acts perpendicular to the potential failure surface, when multiplied by the coefficient of friction (tan ϕ), is equal to the frictional resistance which resists overturning of the slice. The arc length which forms the lower boundary of the slice multiplied by the cohesion is equal to the cohesional resistance to sliding. The total driving force of the potential slide equals the sum of the weight components acting along the failure surface for all of the slices. The total resisting force is equal to the summation of the cohesional and frictional resistance for all of the slices. The ratio of the resisting forces divided by the driving forces is the factor of safety against sliding for the embankment.

The computational portion of the analysis was performed utilizing the ICES Lease (7) computer program. This program was developed to analyze the embankment as a layered system. Numerous potential failure circles are generated until the circle is found which yields the minimum factor of safety.

Three slope stability analyses of the embankment will be presented. The first and second analyses are similar, except that the first analysis does not consider the effects of desiccation while the second analysis does. The third analysis is the analysis used to monitor stability of the embankment during construction.

As presented and discussed in Chapter III, it was determined that there was a slight change in the liquid limit and the percentage of sand with depth. It is common for such changes to occur within a stratum of soil. Sampling is therefore normally conducted near the middle of the soil stratum and the test results are considered to be the average for that stratum. In the first analysis, the data for the upper stratum was obtained from samples taken just below the desiccated zone. Therefore, this analysis did not take into account the increased strength in the upper part of the strata which resulted from desiccation.

After the retesting as described in Chapter III, two analyses were performed. The total stress analyses were performed, utilizing the soil strength as determined from unconsolidated undrained triaxial tests.

In the first analysis, the foundation was considered to consist of two soil strata with the strength in each assumed constant. The triaxial test results presented in Figures 14 and 15 were used to represent these strata. The triaxial test results presented in Figure 8 were used to represent the embankment soils. The analysis did not consider the increased strength near the ground surface as a result of desiccation. The slip circle which produced the lowest factor of safety is presented in Figure 23.

For the second analysis, the upper stratum was divided into three layers and the lower stratum was again considered to be one layer. Therefore, the foundation was divided into a total of four layers to account for the variation in strength with depth. A total stress analysis was performed utilizing the triaxial test results presented in Figures 12, 13, 14, and 15. The slip circle which produced the lowest factor of safety using this method of analysis is presented in Figure 24.

As can be seen in Figure 23, the first analysis which omitted the effects of desiccation yielded a factor of safety of 0.89. A factor of safety which is below one indicates that the embankment is unstable. Thus, the first method of analysis which did not consider the effect of desiccation indicates that the embankment was unsafe and could lead to failure. However, when the increased strength as a result of desiccation was taken into account as in the second analysis, the factor of safety

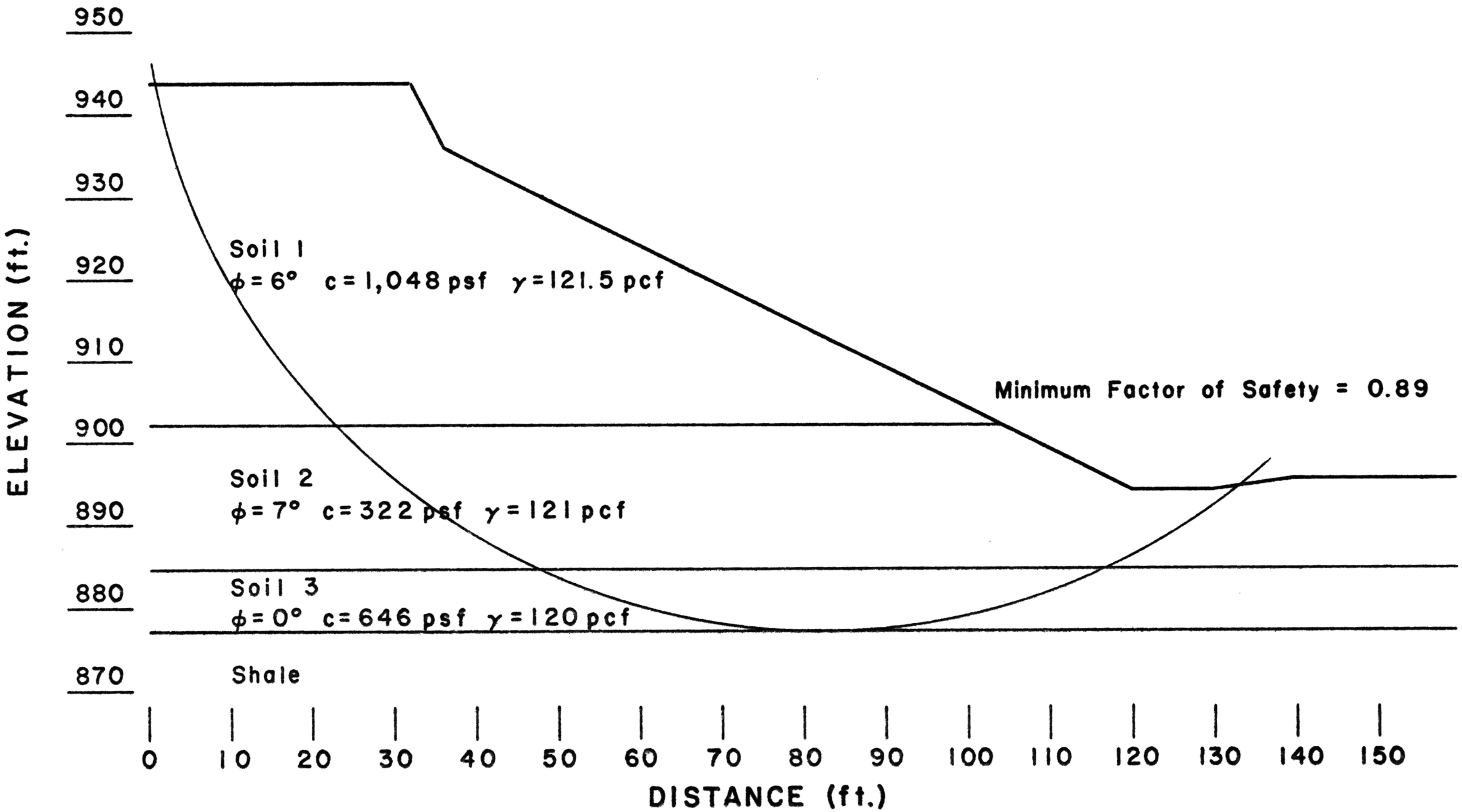

Figure 23. Slope Stability Analysis, Not Considering Desiccation

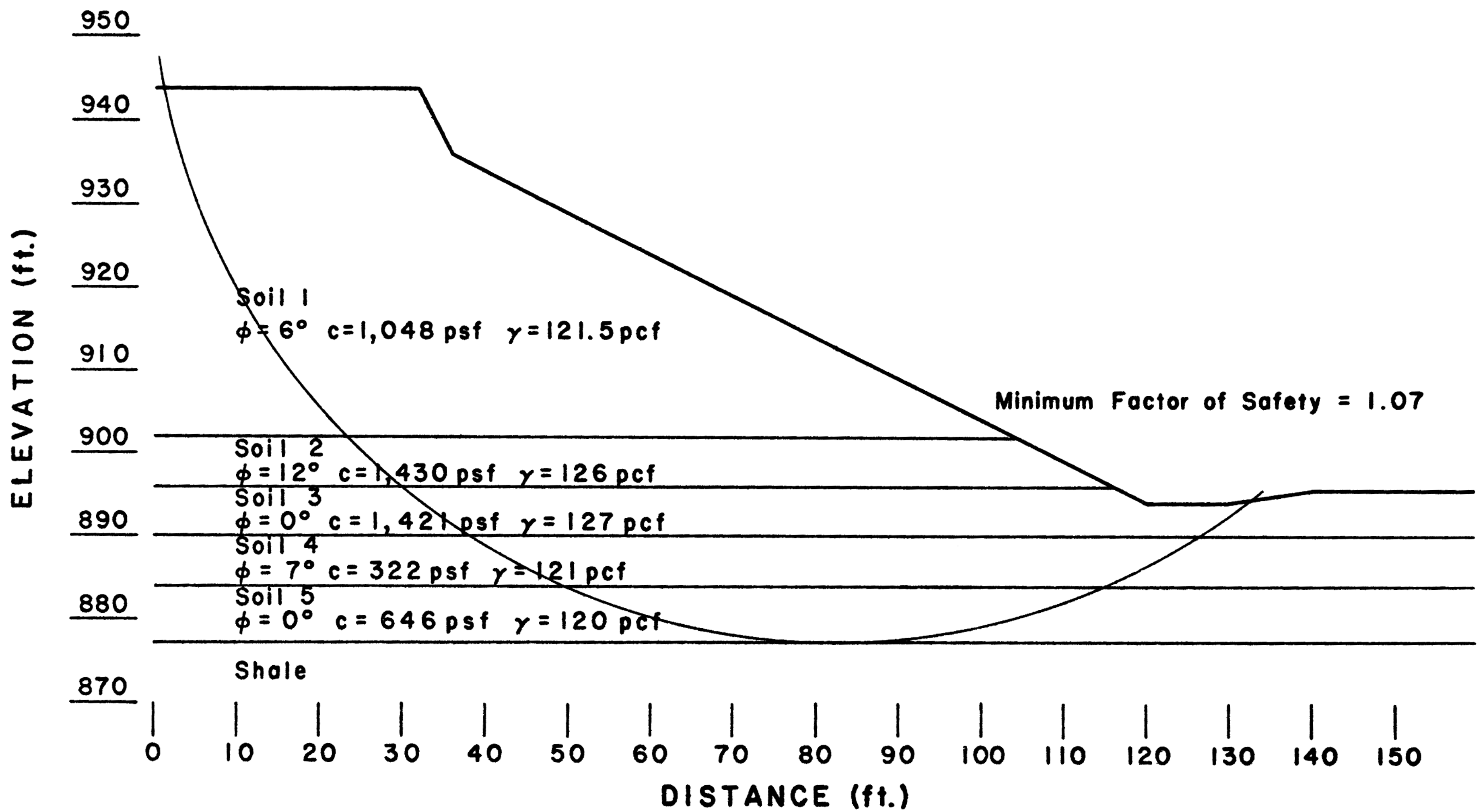

Figure 24. Slope Stability Analysis, Considering Desiccation.

was increased to 1.07, as shown in Figure 24, thus indicating the embankment stability was marginal.

It should be noted that the previously described analyses assumed the worst case loading conditions; this implies that there was no dissipation of excess pore pressure during construction. The third analysis was therefore used to monitor the actual stability of the embankment during construction. This analysis utilized the measured pore pressure presented in Figure 18, in an effective stress analysis. The minimum factor of safety utilizing an effective stress concept was computed to be 1.30. Therefore, the embankment was constructed without any delay since the buildup of excess pore pressure did not reduce the strength below an acceptable level. The measured pore pressure was not as large as anticipated because the water table had been lowered from 3.6 to 8.0 feet below the soil surface as a result of very dry weather in addition to dewatering of the excavations for the bridge piers.

Deformation by Finite Element Analysis

The deformation analysis was performed using the finite element computer program ISBILD (2). This program was developed at the University of California at Berkeley under the sponsorship of the National Science Foundation. The program was developed for the purpose of analyzing the static stresses and strains within an embankment and embankment foundations. The analysis is performed by dividing the structure into a finite number of elements. The individual elements are defined by entering the boundary nodal coordinates and the number of elements desired into the computer program and allowing an internal coordinate generator to define the nodal coordinates. If boundary conditions prevent movement of certain nodal points in either the 'X', 'Y' or both directions, this can be specified as a boundary condition code in the nodal point description.

The program is set up so that all elements are entered as rectangles. By specifying the same nodal point as two corners of the rectangle, a triangle will be generated. A method of utilizing data from conventional laboratory tests is used to describe the stress-strain characteristics of soil. This is accomplished by fitting a hyperbola to the stress-strain curve as developed by Wong and Duncan (8). The description of the material properties then consists of entering the parameters to describe a hyperbola (K,N) which is used to describe the stress-strain characteristics of the soil. Other soil parameters which are entered include the unit weight (UNIT WT), cohesion intercept (C), friction angle (PHI), and Poisson ratio parameters (D,G,F). All of these parameters can be determined from triaxial tests as described in Chapter IV. An example of the input data required to perform this analysis is included in Appendix B.

The program simulates the construction of the embankment by computing the initial foundation stresses and then superimposing the forces on each node corresponding to those developed as a result of the addition of one layer of embankment. The corresponding stresses and strains for all of the elements are determined in two iterations. The first iteration consists of simulating the weight of the newly placed embankment to the foundation soil, however, the newly placed embankment is considered to have no strength. The stress and corresponding strains are computed for this condition. The second iteration considers the strength of the newly placed embankment by modifying the stiffness of the elements used to simulate the embankment. The element stresses and nodal displacements are then recomputed. This process is repeated until the placement of all the embankment layers has been simulated. The element stresses and deformations are printed at the completion of each second iteration.

An example of the output from the computer program is presented in Appendix C. The output consists of nodal displacements and stresses as computed for each element. Only the values corresponding to those of the final layer are presented in Appendix C.

The final displacement consists of those in both X and Y directions (DELTA-X, DELTA-Y), the total displacements in both the X and Y directions (X-DISP, Y-DISP), and the total resultant displacement (TOTAL). The final stresses consist of the normal stress in the X and Y directions (SIG-X, SIG-Y), principal normal stresses (SIG-1, SIG-3), shearing stress in the X-Y direction (TAU-XY), maximum shearing stresses (TAU-MAX), angle of maximum shearing stress (THETA), ratio of principal stresses (SIG1/SIG3), the portion of the available shear strength which is currently mobilized (SLPRES), and the maximum portion of the strength which has been mobilized (SLMAX).

In addition to the output previously described, supporting data is printed for each layer as shown in Appendix D. This output consists of the elastic modulus (ELAS MOD), bulk modulus (BULK MOD), shear modulus (SHEAR MOD), Poisson ratio (POIS), strain in the X and Y directions (EPS-X, EPS-Y), principal strains (EPS-1, EPS-3), unit shearing strains in the XY direction (GAM-XY) and principal unit shearing strain (EPS-1, EPS-3, GAMMAX).

First Finite Element Analysis of the Embankment

In the initial attempt to analyze the embankment, the foundation and the embankment were simulated as separate soils. The element grid pattern used in this analysis is presented in Figure 25. The lower five layers represent the foundation soil and the upper eight layers represent the embankment. As stated previously, the program simulates the placement of the embankment one layer at a time. The final shape of the grid as computed by the program is presented in the overlay for Figure 25.

The vertical line through the foundation soil below the toe of the slope represents the location of the inclinometer casing. Table IX presents computed and measured deflections at various depths along this line.

It should be noted that the excavation at the toe of the fill slope had not been simulated. This could have resulted in larger computed deflections than those shown in the overlay for Figure 25. However, this analysis was not conducted since the computed deflections already greatly exceeded those measured in the field.

Second Finite Element Analysis of the Embankment

The finite element analysis was again performed utilizing the soil parameters obtained from the tests on soil samples taken adjacent to the completed embankment. Four soils were used to simulate the foundation. In this way the variation in strength as a result of desiccation of the upper soil was taken into account.

The computed deflections are presented in Table X along with those measured by the slope inclinometer. Although the second analysis did not

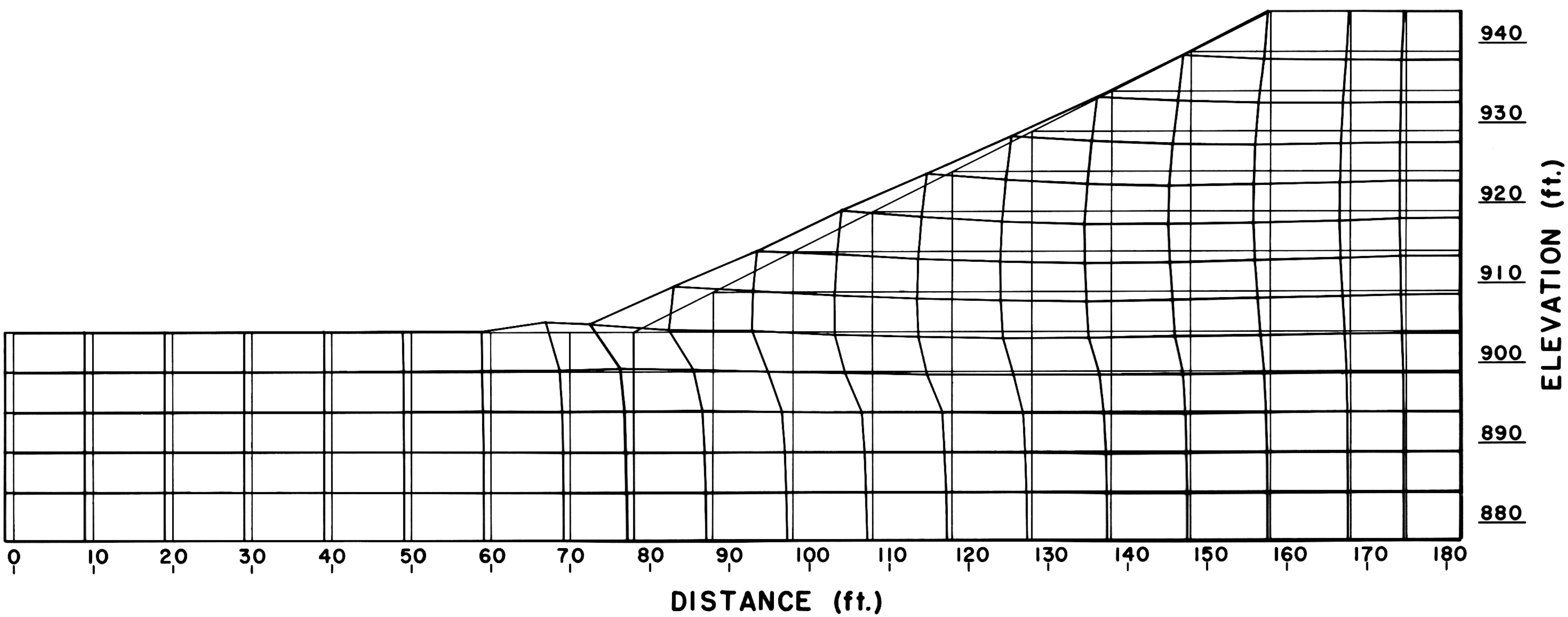

FIGURE 25. Grid for Finite Element Analysis

TABLE IX - DEFLECTIONS COMPUTED NOT CONSIDERING DESICCATION

Depth	Computed Deflection (in.)	Measured Deflection*(in.)
0	57.3	5.3
5	9.8	4.9
10	5.1	3.4
15	2.4	1.6
20	1.1	0.04
26	0.0	-0.03
		*November 15, 1977

TABLE X - DEFLECTIONS COMPUTED CONSIDERING DESICCATION

Depth	Computed Deflection (in.)	Measured Deflection (in.)
0	8.70	5.3
5	8.59	4.9
10	8.51	3.4
15	6.78	1.6
20	4.53	0.04
26	0.00	-0.03

accurately predict the actual magnitude of deflection for the inclinometer, the difference could be attributed to the difference between laboratory and in situ strength parameters.

Effects of Desiccation on Deformation and Slope Stability

A comparison is presented in Figure 26 between the deflections measured by the slope inclinometer and those computed by the use of the finite element analyses. It should be noted that the first analysis indicated that the maximum deflection would occur at the ground surface with considerable deformation within the top ten feet. The actual measurements indicated that the top ten feet of the inclinometer casing remained nearly vertical, but shifted over relative to the bottom of the casing. The major deformation was measured between 10 and 20 feet. It can be seen in Figure 26 that the second analysis predicted the general shape of the deflected inclinometer.

These analyses show the important effect which desiccation has on the deformation. If the soil was normally consolidated, it would be expected that the maximum deformation would occur in the upper strata. The first analysis predicted this type of movement with the predicted displacement decreasing rapidly with depth. However, desiccation caused the upper portion of the soil to be stiffer than the soil below and therefore the soil particles in this portion moved very little relative to each other. The second analysis predicted a deformed shape very similar to that actually measured by the inclinometer.

By properly accounting for desiccation in deformation analyses, more accurate estimates of the deformation can be made. Since accounting for

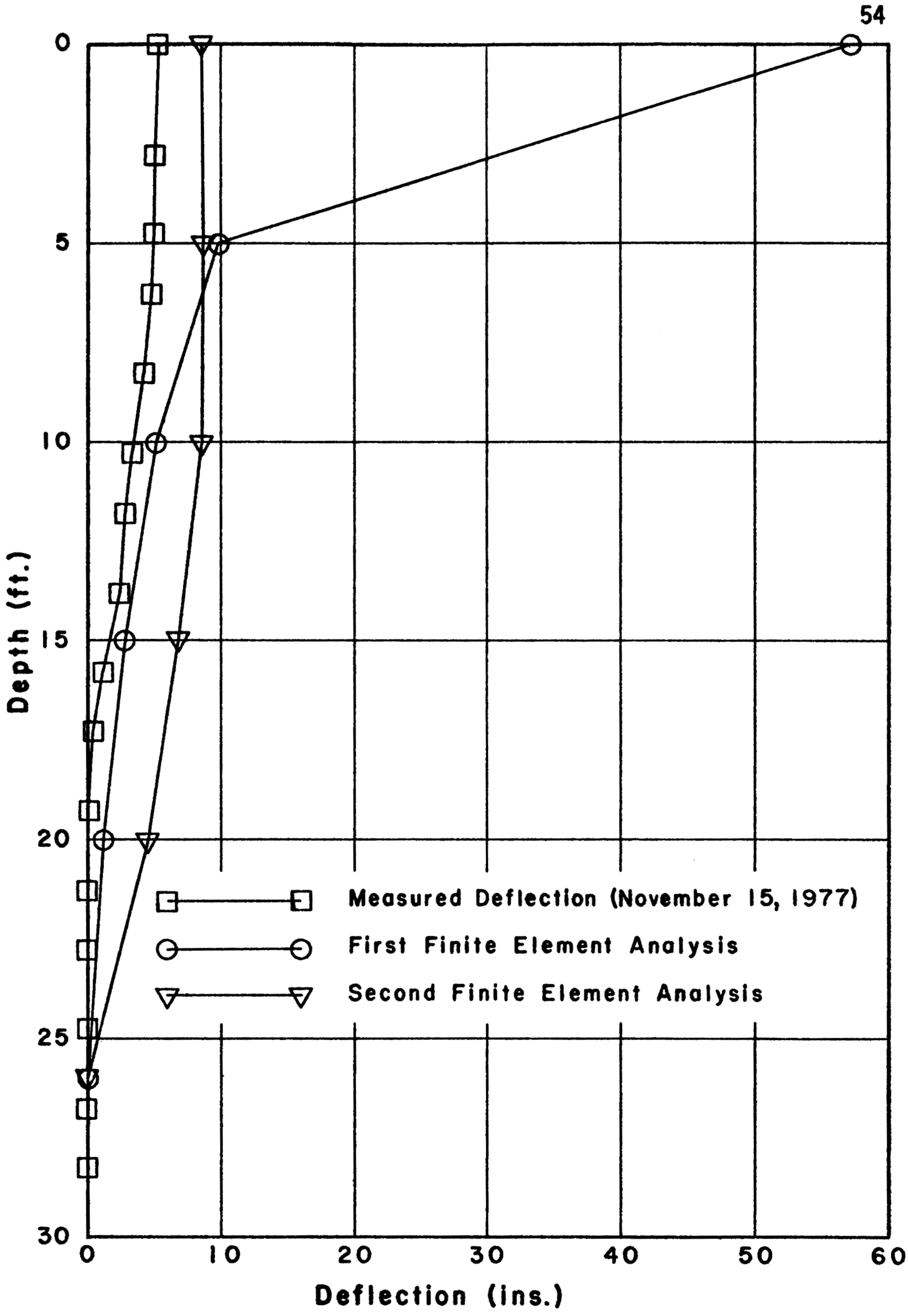

Figure 26. Predicted and Measured Deflections.

desiccation will reduce the magnitude of the expected deformation, the effect on underground structures will not be as severe as would be predicted if desiccation were not considered. Therefore, considerable cost savings may be possible. For example, most underground structures may not be able to withstand the deflection of fifty-seven inches as predicted by the analysis omitting the effects of desiccation. However, they may not be adversely affected by movement of only eight inches as predicted in the analysis considering desiccation. Therefore, the added cost of relocating such structures may be eliminated.

When desiccation was considered in the slope stability analysis, an increase in the factor of safety against sliding from 0.89 to 1.07 was obtained. This resulted in an increase of approximately 25 percent in the factor of safety. By properly accounting for desiccation in the analysis of embankments, it will be possible to design embankments with steeper side slopes, thus providing for additional cost savings.

CHAPTER VI

IDENTIFYING AND ACCOUNTING FOR DESICCATION

The research conducted during this study has shown that the consolidation which results from desiccation has an important influence on the stability of embankments and on the corresponding deformation of the foundation soils. Examples of how desiccation was accounted for in the stability analysis were presented in Chapter V. This was accomplished primarily by dividing the foundation soils into several layers and assigning appropriate strength parameters to the various layers.

The most important step in accounting for desiccation is to recognize the variations in strength and to design the subsurface exploration program such that any variation can be adequately identified. This chapter describes several parameters which should be used in identifying desiccated soils as determined by this study.

Identifying Desiccation

Visually inspecting the soil and recognizing that desiccation has occurred can be very difficult. In the locations examined in this study, the soil had desiccated to a depth of over ten feet at some time in the past. However, at the time of the initial investigation, the groundwater table was at a depth of less than four feet. Since the foundation soil existed in the saturated state, it made recognition of the desiccated soils very difficult.

Moisture tests can aid in determining the depth of desiccation. When desiccation occurs, the negative pore pressure causes consolidation of the soil and therefore a smaller void ratio. When the soil is then resaturated, the water content in the desiccated zone will be lower than for soils in the same stratum, but below the desiccated zone. Therefore, when moisture tests show a sample of soil to have a lower water content than other samples of the soil from lower elevations, the lower water content is a good indication that desiccation has occurred.

The average of the moisture tests run on soil samples from various depths are presented in Table XI. These tests were run on samples taken during the resampling program used for the second finite element analysis. At the time these samples were taken, groundwater stood at a depth of about eight feet.

It can be noted that there is a pronounced increase in the water content between the ten and fifteen foot depths which corresponds to the change from a desiccated to a nondesiccated soil. Since the tests at both ten feet and fifteen feet were below the water table, the change in water content relates directly to the change in void ratio. It should be noted that an increase in water content with depth does not implicitly imply an overconsolidated soil.

A soil index related to the Atterberg Limits which can also be used as an indication of desiccation is the liquidity index. The liquidity index is defined as the difference between the natural water content and the plastic limit divided by the plasticity index. The change in liquidity index is directly related to the change in water content for the soil stratum. For desiccated soils, the liquidity index will be small and

TABLE XI - MOISTURE CONTENTS AT VARIOUS DEPTHS

Depth (Feet)	Water Content (% of Dry Weight)
5	22.7
10	24.5
15	30.0
20	29.75

TABLE XII - LIQUIDITY INDEX AT VARIOUS DEPTHS

Depth	Liquidity Index
5	12
10	25
15	65
20	74

TABLE XIII - DENSITY AT VARIOUS DEPTHS

Depth (Feet)	Average Density (Pounds/Ft^3)
5	103
10	102
15	93
20	92.5

can be negative. For nondesiccated soil, this index will be positive and much larger than for desiccated soils. The liquidity indices for samples from various depths are presented in Table XII. It can be seen that there is an increase of forty in the liquidity index between the ten and fifteen foot depth.

Another factor which could be used to help identify the possible existence of a desiccated zone is the soil density. When desiccation occurs, the negative pore pressure causes consolidation of the soil and therefore an increase in the density. The average densities of the soil at various depths are presented in Table XIII. As in the previously described results, there is a pronounced change at the boundary between the desiccated and nondesiccated zone.

Of the three tests evaluated for identifying the desiccated zone in the field, the density test is probably the best available. However, the density test is much more difficult and also expensive to run than the moisture test. Liquidity index would be very difficult to determine in the field and therefore has less potential as an aid in identifying desiccation so that the sampling locations can be chosen.

The other tests which could be run in the field include Dutch Cone penetrometer, hand van shear, and pocket penetrometer tests. Hand vane shear and pocket penetrometer tests would require removing undisturbed samples for testing. The test results could be plotted to show any variation in strength which may exist as a result of desiccation. Further research should be conducted to evaluate the potential of these tests in identifying desiccation.

CHAPTER VII

CONCLUSIONS AND RECOMMENDATIONS

The primary objective of this research was to determine the effects of desiccation on the deformation and stability of an embankment. Several other important items were also determined. These items included the evaluation of various methods for recognizing desiccated zones of soil. The research objectives were accomplished by comparing the actual deformations which took place under an embankment constructed by the Kansas Department of Transportation with those predicted by using several methods of analysis. From the results obtained from this study, the following can be concluded:

1. Desiccation causes the magnitude of the deformation of the foundation soils to be altered. In the embankment investigated, the maximum deflection predicted without accounting for desiccation in the analysis exceeded the actual deflection by over an order of magnitude. When the effects of desiccation was accounted for in the analysis, the predicted deflection exceeded the measured deflection by only sixty-four percent. The analysis conducted without considering desiccation predicted that the maximum deformation should occur in the upper portion of the foundation soil; however, little deformation was actually measured in this portion.

2. The consideration of desiccation increases the overall stability calculated for embankments constructed over soft foundations. For the embankment analyzed, the computed minimum factor of safety against sliding was increased by approximately 25 percent when desiccation was accounted for in the analysis.
3. Since it is very difficult to recognize the existence of desiccated zones if the groundwater has risen and the soils are resaturated, tests should be performed to aid in their identification. The use of moisture tests, Atterberg limits, and soil density tests are suited for this purpose. The desiccated zone will have a higher density and lower water content than a corresponding zone which is not desiccated. The liquidity index can be used to identify the desiccated zone since this index is sensitive to a variation in natural water content.
4. Reasonably accurate analyses can be performed on desiccated soils by recognizing the variation in strength and choosing the sampling locations in such a way that the soil conditions can be adequately determined and modeled.

With respect to further research regarding the effects of desiccation on deformation and embankment stability, the following recommendations are made:

1. Work should be conducted to further develop procedures for use in the recognition of desiccated zones. Further development of tests are needed which can be used during the initial phase of the field investigation, the results of which are available immediately to aid in the design of the subsurface exploration

program. Such tests as Dutch Cone penetrometer, pocket penetrometer, and hand vane shear should be evaluated in respect to the identification of desiccated zones.

2. Any further work regarding desiccation should include determination of the overconsolidation ratio of the desiccated soil. This will facilitate correlation with other work recorded in the literature.

REFERENCES

1. Terzaghi, Karl, Theoretical Soil Mechanics, John Wiley and Sons, Inc., New York, 1943.

2. Ozawa, Y., and Duncan, J. M., ISBILD: A Computer Program for Analysis of Static Stresses and Movements in Embankments, College of Engineering, Office of Research Services, University of California, Berkeley, California, Report No. TE-73-4, December, 1973.

3. Terzaghi, Karl, and Peck, Ralph B., Soil Mechanics in Engineering Practice, John Wiley and Sons, Inc., New York, 1973, pp. 141-146.

4. Lambe, T. William, and Whitman, Robert V., Soil Mechanics, John Wiley and Sons, Inc., New York, 1969, pp. 451-453.

5. Parry, R. H. G., and Nadarajah, V., Geotechnique, The Institution of Civil Engineers, London, England, Volume 24, Number 3, September, 1974, pp. 345-358.

6. Bishop, A. W., The Use of the Slip Circle in the Stability Analysis of Slopes, Geotechnique, Volume 5, Number 1, 1955.

7. Bailey, William A., and Christian, John T., ICES LEASE - I, A Problem-Oriented Language for Slope Stability Analysis, Soil Mechanics Division and Civil Engineering Systems Laboratory, Department of Civil Engineering, Massachusetts Institute of Technology, Cambridge, Massachusetts, April, 1969.

8. Wong, Kai S., and Duncan, J. M., Hyperbolic Stress-Strain Parameters for Nonlinear Finite Element Analyses of Stresses and Movements in Soil Masses, College of Engineering, Office of Research Services, University of California, Berkeley, California, Report No. TE-74-3, July, 1974.

APPENDIX A

LOG OF BOREHOLE AND REPORT OF SOIL TESTS

SUBSURFACE EXPLORATION AND SAMPLING

Investigation Type: Foundation		Sheet 1 of 1	
Probing Equipment: Bull Soil Sampler		Sampling Equipment: CME 55	
Driller: Marshall	Eng'r: Wineland	Driller: Cavender	Eng'r: Wineland
Date Started: 10-3-73	Date Completed: 10-3-73	Date Started: 10-4-73	Date Completed: 10-4-73

Proj. No. 70-89 I 70-5 (55)
Location: I-70 and Gage Interchange

Material Type: Sand, Silt, Clay, Shale, Limestone, Other

Field Test Type: PP = Pocket Penetrometer; TV = Torvane Shear Device (tsf); SPT = Standard Penetration (blows/foot)

Sample Condition: G = Good; F = Fair; P = Poor; L = Lost; D = Disturbed; S = Saturated; U = Unstable; R = Roots; C = Cracked; B = Broken

PROBE DATA

Hole Number: 1
Station: 77+52 ℄ Distance: 30' Rt.
Top Hole Elevation: 902.2

Depth Elev. (ft.)	Classification and Description of Materials, Comments	Ident.
0 – 1.2	Silty Clay Loam P.I. = 15 Very dark gray, 10 YR 3/1	2-1
1.2 – 2.8	Clay P.I. = 11 Dark brown, 7.5 YR 4/4 Contains iron stone nodules	1-2
2.8 – 17.6	Silty Clay P.I. = 20 Dark gray, 10 YR 4/1	1-T
17.6 – 24.8	Clay Loam P.I. = 13	1
24.8 –	Severy Shale	

SAMPLE DATA

Hole No.	Sample Number	Depth of Retained Sample	Condition	Pushed/Rec.
1A	1-T	10.1 – 10.8		
1A	1C-3A	19.0 – 19.7		
1B	2-T	10.8 – 11.4		
1B	1C-3B	20.7 – 21.4		
1C	3-T	11.7 – 12.4		
1C	1C-3C	22.2 – 22.9		

3.8' ▽ 24 hr. Water level

1-1om-73-1500

S.H.C. Form No. 1139

STATE HIGHWAY COMMISSION OF KANSAS

REPORT OF SOIL TESTS

SUBMITTED BY J. D. Wineland ADDRESS Topeka LAB. NO.

PROJECT 70-89 I 70-5 (55) COUNTY Shawnee DATE

MECHANICAL ANALYSIS

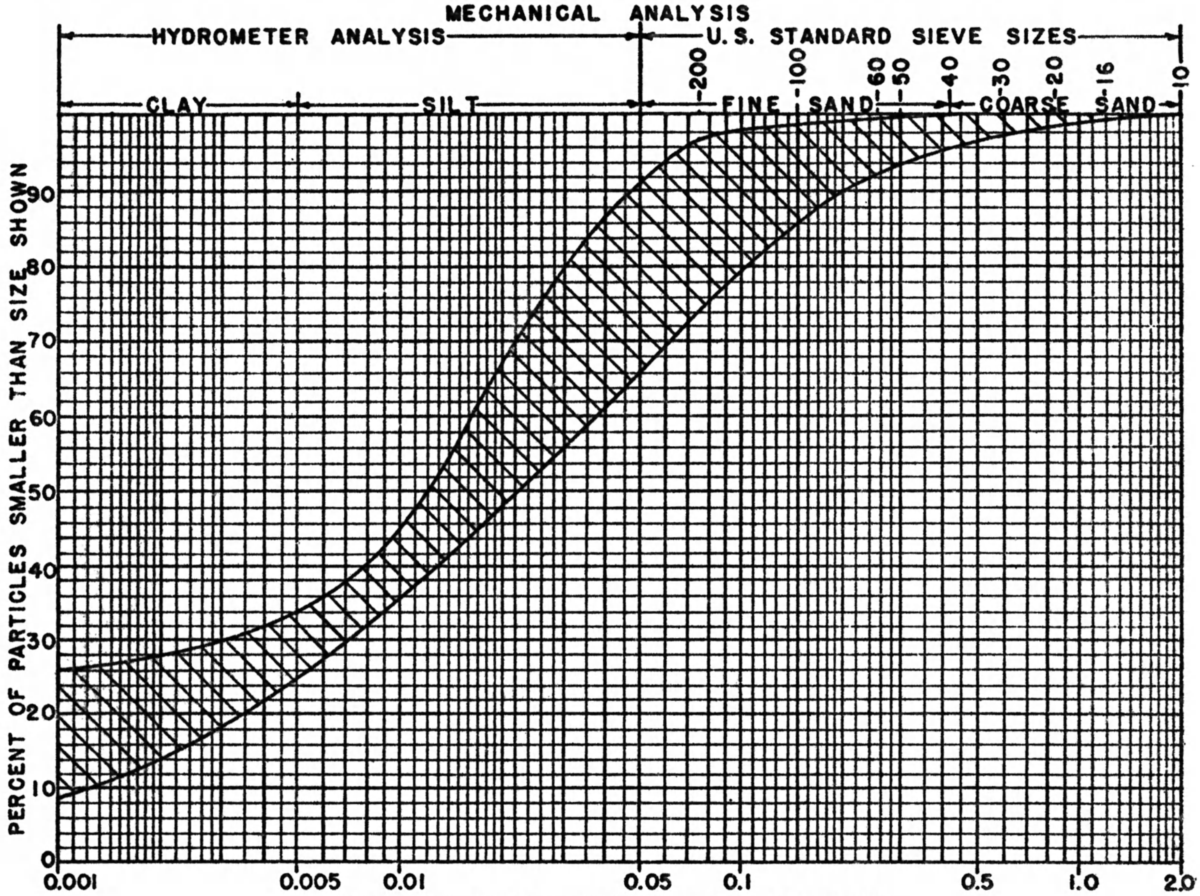

PHYSICAL PROPERTIES OF PORTION PASSING NO.___SIEVE

SAMPLE NUMBER	STATION	DIST. ₵	DEPTH	* L.L.L.	* L.P.L.	* P.I.	% RET. ON NO.10	SPEC. GRAV. (PASS. NO.10)	CLASSI-FICATION
				37.3	20.2	17.1		2.64	

REMARKS *Average test results.

ENG'R. OF MATERIALS

BY

STATE HIGHWAY COMMISSION OF KANSAS

REPORT OF SOIL TESTS

SUBMITTED BY *J. D. Wineland* ADDRESS *Topeka* LAB. NO. ____

PROJECT *70-89 I 70-5 (55)* COUNTY *Shawnee* DATE ____

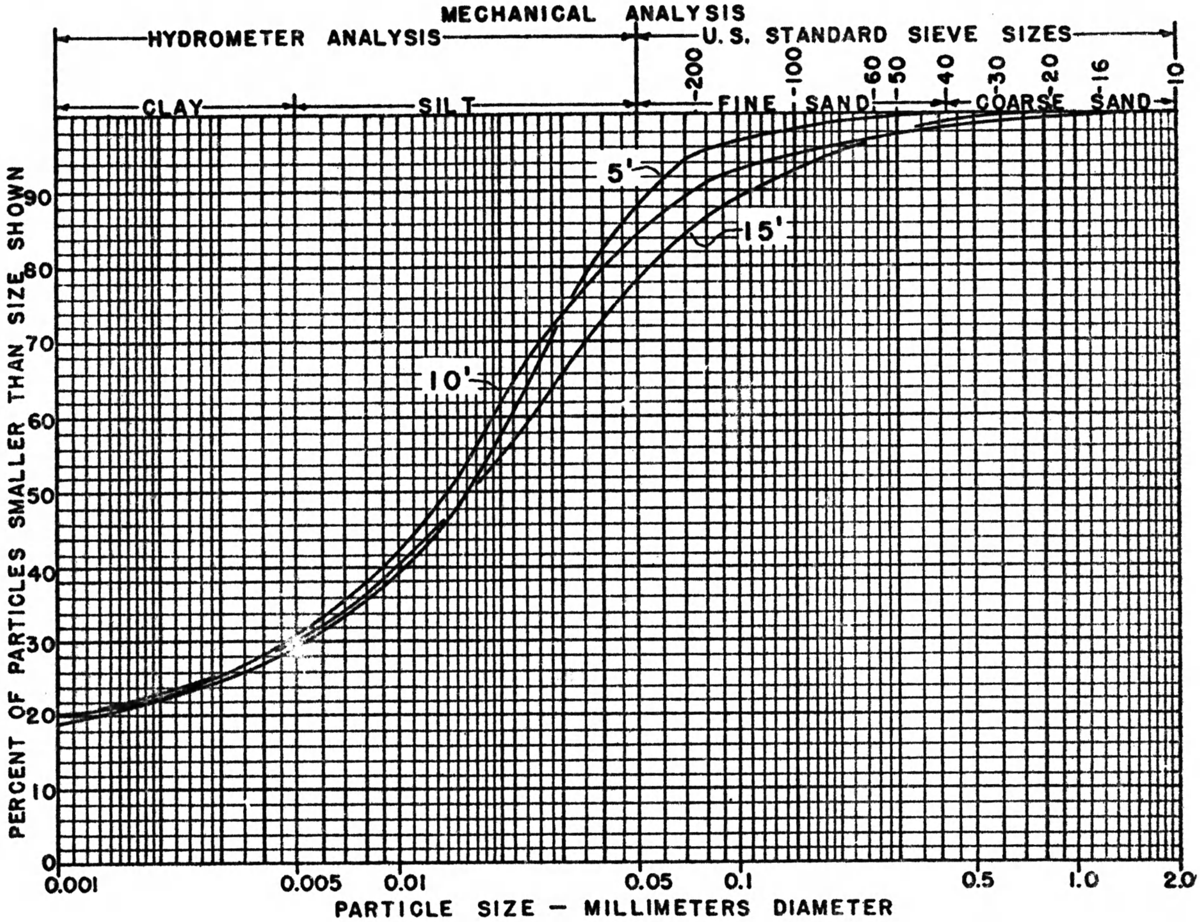

PHYSICAL PROPERTIES OF PORTION PASSING NO.___SIEVE

SAMPLE NUMBER	STATION	DIST. ℄	DEPTH	* L.L.L.	* L.P.L.	* P.I.	% RET. ON NO.10	SPEC. GRAV. (PASS. NO.10)	CLASSI- FICATION
			5'	*39.0*	*20.5*	*18.5*	*0*	*2.63*	*SiCL*
			10'	*38.6*	*19.8*	*18.8*	*0*	*2.66*	*SiC*
			15'	*35.3*	*20.3*	*15.0*	*0*	*2.64*	*C*

REMARKS **Average test results.*

ENG'R. OF MATERIALS

BY ____

33-1082-8—6-28 9-69-5M

S. H. C. Form No. 635

APPENDIX B

INPUT FOR THE FINITE ELEMENT COMPUTER PROGRAM

I 70 AND GAGE ONE HALF EMBANKMENT FOUNDATION STRESS GENERATED

TOTAL NUMBER OF ELEMENTS**********155

TOTAL NUMBER OF NODES*************180

NUMBER OF ELEMENTS IN FOUNDATION** 95

NUMBER OF NODES IN FOUNDATION*****120

NUMBER OF PREEXISTING ELEMENTS**** 0

NUMBER OF PREEXISTING NODES******* 0

NUMBER OF DIFF. MATERIALS********* 5

NUMBER OF CONSTRUCTION LAYERS***** 8

NUMBER OF LOAD CASES************** 0

FINAL RESULTS ARE NOT PUNCHED OUT

MATERIAL PROPERTY DATA

ATMOSPHERIC PRESSURE=   2.1160

MAT	UNIT WT	K	MODULUS KUR	N	D	POISSON RATIO G	F	C	PHI	FAIL.RATIO	KO
1	0.1200	97.0	290.9	-1.1733	0.0	0.5000	0.0	0.6460	0.0	0.9550	1.0000
2	0.1210	57.9	173.6	0.2724	0.0	0.5000	0.0	0.3220	7.0700	0.9240	1.0000
3	0.1250	445.5	1336.5	-0.1728	0.0	0.5000	0.0	1.4210	0.0	1.0210	1.0000
4	0.1260	187.2	561.6	0.2445	0.0	0.5000	0.0	1.4300	11.5800	0.9527	1.0000
5	0.1190	102.2	306.6	0.2650	0.0	0.5000	0.0	3.3400	15.0000	0.6011	0.0

NODAL POINT INPUT DATA

NODE NUMBER	NODAL POINT COORDINATES X-ORD	Y-ORD	B.C. CODE XX	YY
1	0.0	878.000	1	1
2	10.000	878.000	1	1
3	20.000	878.000	1	1
4	30.000	878.000	1	1
5	40.000	878.000	1	1
6	50.000	878.000	1	1
7	60.000	878.000	1	1
8	70.000	878.000	1	1
9	78.000	878.000	1	1
10	88.000	878.000	1	1
11	98.000	878.000	1	1
12	108.000	878.000	1	1
13	118.000	878.000	1	1
14	128.000	878.000	1	1
15	138.000	878.000	1	1
16	148.000	878.000	1	1
17	158.000	878.000	1	1
18	168.000	878.000	1	1
19	175.000	878.000	1	1
20	182.000	878.000	1	1
21	0.0	884.000	1	0
22	10.000	884.000	0	0
23	20.000	884.000	0	0
24	30.000	884.000	0	0
25	40.000	884.000	0	0
26	50.000	884.000	0	0
27	60.000	884.000	0	0
28	70.000	884.000	0	0
29	78.000	884.000	0	0
30	88.000	884.000	0	0
31	98.000	884.000	0	0
32	108.000	884.000	0	0
33	118.000	884.000	0	0
34	128.000	884.000	0	0
35	138.000	884.000	0	0
36	148.000	884.000	0	0
37	158.000	884.000	0	0
38	168.000	884.000	0	0
39	175.000	884.000	0	0
40	182.000	884.000	1	0
41	0.0	889.000	1	0
42	10.000	889.000	0	0
43	20.000	889.000	0	0
44	30.000	889.000	0	0
45	40.000	889.000	0	0
46	50.000	889.000	0	0
47	60.000	889.000	0	0
48	70.000	889.000	0	0
49	78.000	889.000	0	0
50	88.000	889.000	0	0
51	98.000	889.000	0	0
52	108.000	889.000	0	0
53	118.000	889.000	0	0
54	128.000	889.000	0	0
55	138.000	889.000	0	0

56	148.000	889.000	0	0
57	158.000	889.000	0	0
58	168.000	889.000	0	0
59	175.000	889.000	0	0
60	182.000	889.000	1	0
61	0.0	894.000	1	0
62	10.000	894.000	0	0
63	20.000	894.000	0	0
64	30.000	894.000	0	0
65	40.000	894.000	0	0
66	50.000	894.000	0	0
67	60.000	894.000	0	0
68	70.000	894.000	0	0
69	78.000	894.000	0	0
70	88.000	894.000	0	0
71	98.000	894.000	0	0
72	108.000	894.000	0	0
73	118.000	894.000	0	0
74	128.000	894.000	0	0
75	138.000	894.000	0	0
76	148.000	894.000	0	0
77	158.000	894.000	0	0
78	168.000	894.000	0	0
79	175.000	894.000	0	0
80	182.000	894.000	1	0
81	0.0	899.000	1	0
82	10.000	899.000	0	0
83	20.000	899.000	0	0
84	30.000	899.000	0	0
85	40.000	899.000	0	0
86	50.000	899.000	0	0
87	60.000	899.000	0	0
88	70.000	899.000	0	0
89	78.000	899.000	0	0
90	88.000	899.000	0	0
91	98.000	899.000	0	0
92	108.000	899.000	0	0
93	118.000	899.000	0	0
94	128.000	899.000	0	0
95	138.000	899.000	0	0
96	148.000	899.000	0	0
97	158.000	899.000	0	0
98	168.000	899.000	0	0
99	175.000	899.000	0	0
100	182.000	899.000	1	0
101	0.0	904.000	1	0
102	10.000	904.000	0	0
103	20.000	904.000	0	0
104	30.000	904.000	0	0
105	40.000	904.000	0	0
106	50.000	904.000	0	0
107	60.000	904.000	0	0
108	70.000	904.000	0	0
109	78.000	904.000	0	0
110	88.000	904.000	0	0
111	98.000	904.000	0	0
112	108.000	904.000	0	0
113	118.000	904.000	0	0
114	128.000	904.000	0	0
115	138.000	904.000	0	0

116	148.000	904.000	0	0
117	158.000	904.000	0	0
118	168.000	904.000	0	0
119	175.000	904.000	0	0
120	182.000	904.000	1	0
121	88.000	909.000	0	0
122	98.000	909.000	0	0
123	108.000	909.000	0	0
124	118.000	909.000	0	0
125	128.000	909.000	0	0
126	138.000	909.000	0	0
127	148.000	909.000	0	0
128	158.000	909.000	0	0
129	168.000	909.000	0	0
130	175.000	909.000	0	0
131	182.000	909.000	1	0
132	98.000	914.000	0	0
133	108.000	914.000	0	0
134	118.000	914.000	0	0
135	128.000	914.000	0	0
136	138.000	914.000	0	0
137	148.000	914.000	0	0
138	158.000	914.000	0	0
139	168.000	914.000	0	0
140	175.000	914.000	0	0
141	182.000	914.000	1	0
142	108.000	919.000	0	0
143	118.000	919.000	0	0
144	128.000	919.000	0	0
145	138.000	919.000	0	0
146	148.000	919.000	0	0
147	158.000	919.000	0	0
148	168.000	919.000	0	0
149	175.000	919.000	0	0
150	182.000	919.000	1	0
151	118.000	924.000	0	0
152	128.000	924.000	0	0
153	138.000	924.000	0	0
154	148.000	924.000	0	0
155	158.000	924.000	0	0
156	168.000	924.000	0	0
157	175.000	924.000	0	0
158	182.000	924.000	1	0
159	128.000	929.000	0	0
160	138.000	929.000	0	0
161	148.000	929.000	0	0
162	158.000	929.000	0	0
163	168.000	929.000	0	0
164	175.000	929.000	0	0
165	182.000	929.000	1	0
166	138.000	934.000	0	0
167	148.000	934.000	0	0
168	158.000	934.000	0	0
169	168.000	934.000	0	0
170	175.000	934.000	0	0
171	182.000	934.000	1	0
172	148.000	939.000	0	0
173	158.000	939.000	0	0
174	168.000	939.000	0	0
175	175.000	939.000	0	0

176	182.000	939.000	1	0
177	158.000	944.000	0	0
178	168.000	944.000	0	0
179	175.000	944.000	0	0
180	182.000	944.000	1	0

FOUR NODES SOLID ELEMENT DATA

ELEMT NO.	CONNECTED NODES I	J	K	L	MATL NO.	ELEMENT CENTER COORDINATES X-ORD	Y-ORD
1	1	2	22	21	1	5.000	881.000
2	2	3	23	22	1	15.000	881.000
3	3	4	24	23	1	25.000	881.000
4	4	5	25	24	1	35.000	881.000
5	5	6	26	25	1	45.000	881.000
6	6	7	27	26	1	55.000	881.000
7	7	8	28	27	1	65.000	881.000
8	8	9	29	28	1	74.000	881.000
9	9	10	30	29	1	83.000	881.000
10	10	11	31	30	1	93.000	881.000
11	11	12	32	31	1	103.000	881.000
12	12	13	33	32	1	113.000	881.000
13	13	14	34	33	1	123.000	881.000
14	14	15	35	34	1	133.000	881.000
15	15	16	36	35	1	143.000	881.000
16	16	17	37	36	1	153.000	881.000
17	17	18	38	37	1	163.000	881.000
18	18	19	39	38	1	171.500	881.000
19	19	20	40	39	1	178.500	881.000
20	21	22	42	41	1	5.000	886.500
21	22	23	43	42	1	15.000	886.500
22	23	24	44	43	1	25.000	886.500
23	24	25	45	44	1	35.000	886.500
24	25	26	46	45	1	45.000	886.500
25	26	27	47	46	1	55.000	886.500
26	27	28	48	47	1	65.000	886.500
27	28	29	49	48	1	74.000	886.500
28	29	30	50	49	1	83.000	886.500
29	30	31	51	50	1	93.000	886.500
30	31	32	52	51	1	103.000	886.500
31	32	33	53	52	1	113.000	886.500
32	33	34	54	53	1	123.000	886.500
33	34	35	55	54	1	133.000	886.500
34	35	36	56	55	1	143.000	886.500
35	36	37	57	56	1	153.000	886.500
36	37	38	58	57	1	163.000	886.500
37	38	39	59	58	1	171.500	886.500
38	39	40	60	59	1	178.500	886.500
39	41	42	62	61	2	5.000	891.500
40	42	43	63	62	2	15.000	891.500
41	43	44	64	63	2	25.000	891.500
42	44	45	65	64	2	35.000	891.500
43	45	46	66	65	2	45.000	891.500
44	46	47	67	66	2	55.000	891.500
45	47	48	68	67	2	65.000	891.500
46	48	49	69	68	2	74.000	891.500
47	49	50	70	69	2	83.000	891.500
48	50	51	71	70	2	93.000	891.500
49	51	52	72	71	2	103.000	891.500
50	52	53	73	72	2	113.000	891.500
51	53	54	74	73	2	123.000	891.500
52	54	55	75	74	2	133.000	891.500
53	55	56	76	75	2	143.000	891.500
54	56	57	77	76	2	153.000	891.500
55	57	58	78	77	2	163.000	891.500

56	58	59	79	78	2	171.500	891.500
57	59	60	80	79	2	178.500	891.500
58	61	62	82	81	3	5.000	896.500
59	62	63	83	82	3	15.000	896.500
60	63	64	84	83	3	25.000	896.500
61	64	65	85	84	3	35.000	896.500
62	65	66	86	85	3	45.000	896.500
63	66	67	87	86	3	55.000	896.500
64	67	68	88	87	3	65.000	896.500
65	68	69	89	88	3	74.000	896.500
66	69	70	90	89	3	83.000	896.500
67	70	71	91	90	3	93.000	896.500
68	71	72	92	91	3	103.000	896.500
69	72	73	93	92	3	113.000	896.500
70	73	74	94	93	3	123.000	896.500
71	74	75	95	94	3	133.000	896.500
72	75	76	96	95	3	143.000	896.500
73	76	77	97	96	3	153.000	896.500
74	77	78	98	97	3	163.000	896.500
75	78	79	99	98	3	171.500	896.500
76	79	80	100	99	3	178.500	896.500
77	81	82	102	101	4	5.000	901.500
78	82	83	103	102	4	15.000	901.500
79	83	84	104	103	4	25.000	901.500
80	84	85	105	104	4	35.000	901.500
81	85	86	106	105	4	45.000	901.500
82	86	87	107	106	4	55.000	901.500
83	87	88	108	107	4	65.000	901.500
84	88	89	109	108	4	74.000	901.500
85	89	90	110	109	4	83.000	901.500
86	90	91	111	110	4	93.000	901.500
87	91	92	112	111	4	103.000	901.500
88	92	93	113	112	4	113.000	901.500
89	93	94	114	113	4	123.000	901.500
90	94	95	115	114	4	133.000	901.500
91	95	96	116	115	4	143.000	901.500
92	96	97	117	116	4	153.000	901.500
93	97	98	118	117	4	163.000	901.500
94	98	99	119	118	4	171.500	901.500
95	99	100	120	119	4	178.500	901.500
96	109	110	121	121	5	85.500	906.500
97	110	111	122	121	5	93.000	906.500
98	111	112	123	122	5	103.000	906.500
99	112	113	124	123	5	113.000	906.500
100	113	114	125	124	5	123.000	906.500
101	114	115	126	125	5	133.000	906.500
102	115	116	127	126	5	143.000	906.500
103	116	117	128	127	5	153.000	906.500
104	117	118	129	128	5	163.000	906.500
105	118	119	130	129	5	171.500	906.500
106	119	120	131	130	5	178.500	906.500
107	121	122	132	132	5	95.500	911.500
108	122	123	133	132	5	103.000	911.500
109	123	124	134	133	5	113.000	911.500
110	124	125	135	134	5	123.000	911.500
111	125	126	136	135	5	133.000	911.500
112	126	127	137	136	5	143.000	911.500
113	127	128	138	137	5	153.000	911.500
114	128	129	139	138	5	163.000	911.500
115	129	130	140	139	5	171.500	911.500

116	130	131	141	140	5	178.500	911.500
117	132	133	142	142	5	105.500	916.500
118	133	134	143	142	5	113.000	916.500
119	134	135	144	143	5	123.000	916.500
120	135	136	145	144	5	133.000	916.500
121	136	137	146	145	5	143.000	916.500
122	137	138	147	146	5	153.000	916.500
123	138	139	148	147	5	163.000	916.500
124	139	140	149	148	5	171.500	916.500
125	140	141	150	149	5	178.500	916.500
126	142	143	151	151	5	115.500	921.500
127	143	144	152	151	5	123.000	921.500
128	144	145	153	152	5	133.000	921.500
129	145	146	154	153	5	143.000	921.500
130	146	147	155	154	5	153.000	921.500
131	147	148	156	155	5	163.000	921.500
132	148	149	157	156	5	171.500	921.500
133	149	150	158	157	5	178.500	921.500
134	151	152	159	159	5	125.500	926.500
135	152	153	160	159	5	133.000	926.500
136	153	154	161	160	5	143.000	926.500
137	154	155	162	161	5	153.000	926.500
138	155	156	163	162	5	163.000	926.500
139	156	157	164	163	5	171.500	926.500
140	157	158	165	164	5	178.500	926.500
141	159	160	166	166	5	135.500	931.500
142	160	161	167	166	5	143.000	931.500
143	161	162	168	167	5	153.000	931.500
144	162	163	169	168	5	163.000	931.500
145	163	164	170	169	5	171.500	931.500
146	164	165	171	170	5	178.500	931.500
147	166	167	172	172	5	145.500	936.500
148	167	168	173	172	5	153.000	936.500
149	168	169	174	173	5	163.000	936.500
150	169	170	175	174	5	171.500	936.500
151	170	171	176	175	5	178.500	936.500
152	172	173	177	177	5	155.500	941.500
153	173	174	178	177	5	163.000	941.500
154	174	175	179	178	5	171.500	941.500
155	175	176	180	179	5	178.500	941.500

APPENDIX C

OUTPUT FOR THE FINITE ELEMENT COMPUTER PROGRAM

LAYER NUMBER = 8   ITERATION = 2
****

NP	DELTA-X	DELTA-Y	X-DISP	Y-DISP	TOTAL	NP
1	0.0	0.0	0.0	0.0	0.0	1
2	0.0	0.0	0.0	0.0	0.0	2
3	0.0	0.0	0.0	0.0	0.0	3
4	0.0	0.0	0.0	0.0	0.0	4
5	0.0	0.0	0.0	0.0	0.0	5
6	0.0	0.0	0.0	0.0	0.0	6
7	0.0	0.0	0.0	0.0	0.0	7
8	0.0	0.0	0.0	0.0	0.0	8
9	0.0	0.0	0.0	0.0	0.0	9
10	0.0	0.0	0.0	0.0	0.0	10
11	0.0	0.0	0.0	0.0	0.0	11
12	0.0	0.0	0.0	0.0	0.0	12
13	0.0	0.0	0.0	0.0	0.0	13
14	0.0	0.0	0.0	0.0	0.0	14
15	0.0	0.0	0.0	0.0	0.0	15
16	0.0	0.0	0.0	0.0	0.0	16
17	0.0	0.0	0.0	0.0	0.0	17
18	0.0	0.0	0.0	0.0	0.0	18
19	0.0	0.0	0.0	0.0	0.0	19
20	0.0	0.0	0.0	0.0	0.0	20
21	0.0	0.0002	0.0	0.0027	0.0027	21
22	-0.0011	0.0003	-0.0110	0.0029	0.0114	22
23	-0.0023	0.0003	-0.0228	0.0030	0.0229	23
24	-0.0038	0.0005	-0.0360	0.0039	0.0362	24
25	-0.0060	0.0007	-0.0546	0.0063	0.0549	25
26	-0.0103	0.0019	-0.0887	0.0138	0.0898	26
27	-0.0196	0.0034	-0.1537	0.0241	0.1556	27
28	-0.0368	0.0069	-0.2580	0.0356	0.2605	28
29	-0.0618	0.0103	-0.3779	0.0446	0.3806	29
30	-0.1112	0.0211	-0.5610	0.0553	0.5637	30
31	-0.1723	0.0180	-0.7374	0.0375	0.7384	31
32	-0.2206	0.0242	-0.8443	0.0183	0.8445	32
33	-0.2286	0.0010	-0.8518	-0.0399	0.8528	33
34	-0.2300	-0.0264	-0.7848	-0.0968	0.7908	34
35	-0.2065	-0.0348	-0.6523	-0.1121	0.6619	35
36	-0.1605	-0.0349	-0.4882	-0.1076	0.5000	36
37	-0.1085	-0.0298	-0.3257	-0.0941	0.3390	37
38	-0.0564	-0.0245	-0.1742	-0.0803	0.1919	38
39	-0.0254	-0.0180	-0.0820	-0.0680	0.1065	39
40	0.0	-0.0161	0.0	-0.0639	0.0639	40
41	0.0	0.0010	0.0	0.0098	0.0098	41
42	-0.0021	0.0010	-0.0192	0.0099	0.0216	42
43	-0.0044	0.0013	-0.0395	0.0109	0.0409	43
44	-0.0072	0.0015	-0.0627	0.0130	0.0641	44
45	-0.0119	0.0030	-0.0964	0.0221	0.0989	45
46	-0.0211	0.0062	-0.1561	0.0432	0.1620	46
47	-0.0391	0.0126	-0.2606	0.0771	0.2717	47
48	-0.0707	0.0208	-0.4184	0.1071	0.4319	48
49	-0.1054	0.0330	-0.5654	0.1321	0.5807	49
50	-0.1545	0.0455	-0.7452	0.1378	0.7579	50
51	-0.1949	0.0443	-0.8716	0.0970	0.8770	51
52	-0.2109	0.0287	-0.9247	0.0244	0.9250	52
53	-0.2143	0.0023	-0.9068	-0.0693	0.9095	53
54	-0.2155	-0.0266	-0.8594	-0.1531	0.8730	54

55	-0.2147	-0.0552	-0.7774	-0.2098	0.8053	55
56	-0.1956	-0.0622	-0.6474	-0.2186	0.6833	56
57	-0.1565	-0.0670	-0.4799	-0.2163	0.5264	57
58	-0.0986	-0.0633	-0.2878	-0.2001	0.3505	58
59	-0.0504	-0.0560	-0.1448	-0.1842	0.2343	59
60	0.0	-0.0519	0.0	-0.1763	0.1763	60
61	0.0	0.0023	0.0	0.0219	0.0219	61
62	-0.0039	0.0025	-0.0335	0.0227	0.0405	62
63	-0.0084	0.0029	-0.0700	0.0249	0.0743	63
64	-0.0144	0.0040	-0.1132	0.0306	0.1172	64
65	-0.0225	0.0066	-0.1672	0.0464	0.1735	65
66	-0.0364	0.0139	-0.2455	0.0862	0.2602	66
67	-0.0604	0.0250	-0.3697	0.1446	0.3970	67
68	-0.0976	0.0419	-0.5450	0.1997	0.5804	68
69	-0.1373	0.0560	-0.7090	0.2224	0.7431	69
70	-0.1738	0.0644	-0.8434	0.1953	0.8657	70
71	-0.1911	0.0535	-0.9020	0.1224	0.9103	71
72	-0.1980	0.0306	-0.9073	0.0169	0.9074	72
73	-0.1993	0.0027	-0.8886	-0.0927	0.8934	73
74	-0.2001	-0.0262	-0.8475	-0.1905	0.8686	74
75	-0.2005	-0.0562	-0.7826	-0.2679	0.8272	75
76	-0.1939	-0.0777	-0.6747	-0.3076	0.7416	76
77	-0.1618	-0.0929	-0.5154	-0.3234	0.6084	77
78	-0.1081	-0.1005	-0.3194	-0.3225	0.4539	78
79	-0.0579	-0.0979	-0.1648	-0.3121	0.3529	79
80	0.0	-0.0968	0.0	-0.3081	0.3081	80
81	0.0	0.0043	0.0	0.0386	0.0386	81
82	-0.0048	0.0047	-0.0377	0.0402	0.0551	82
83	-0.0107	0.0057	-0.0799	0.0452	0.0918	83
84	-0.0185	0.0079	-0.1320	0.0560	0.1434	84
85	-0.0310	0.0127	-0.2033	0.0812	0.2189	85
86	-0.0501	0.0236	-0.3013	0.1361	0.3306	86
87	-0.0811	0.0419	-0.4385	0.2209	0.4910	87
88	-0.1194	0.0609	-0.6053	0.2865	0.6697	88
89	-0.1452	0.0769	-0.7157	0.3003	0.7762	89
90	-0.1712	0.0733	-0.8195	0.2305	0.8513	90
91	-0.1804	0.0576	-0.8521	0.1304	0.8620	91
92	-0.1839	0.0314	-0.8567	0.0121	0.8567	92
93	-0.1849	0.0030	-0.8415	-0.1066	0.8482	93
94	-0.1853	-0.0259	-0.8098	-0.2162	0.8382	94
95	-0.1853	-0.0563	-0.7481	-0.3142	0.8114	95
96	-0.1772	-0.0902	-0.6449	-0.3859	0.7515	96
97	-0.1480	-0.1214	-0.4917	-0.4301	0.6533	97
98	-0.0975	-0.1416	-0.3027	-0.4477	0.5435	98
99	-0.0514	-0.1483	-0.1546	-0.4497	0.4755	99
100	0.0	-0.1502	0.0	-0.4492	0.4492	100
101	0.0	0.0067	0.0	0.0571	0.0571	101
102	-0.0056	0.0073	-0.0417	0.0598	0.0729	102
103	-0.0123	0.0091	-0.0887	0.0685	0.1121	103
104	-0.0221	0.0130	-0.1499	0.0871	0.1734	104
105	-0.0371	0.0208	-0.2345	0.1250	0.2657	105
106	-0.0615	0.0364	-0.3518	0.1957	0.4026	106
107	-0.0929	0.0591	-0.4871	0.2922	0.5680	107
108	-0.1299	0.0798	-0.6262	0.3622	0.7234	108
109	-0.1526	0.0869	-0.7248	0.3491	0.8045	109
110	-0.1603	0.0797	-0.7801	0.2577	0.8216	110
111	-0.1682	0.0592	-0.8232	0.1365	0.8344	111
112	-0.1692	0.0321	-0.8242	0.0057	0.8242	112
113	-0.1704	0.0034	-0.8092	-0.1198	0.8180	113
114	-0.1709	-0.0259	-0.7705	-0.2431	0.8079	114

115	-0.1692	-0.0573	-0.7068	-0.3566	0.7916	115
116	-0.1566	-0.1008	-0.6023	-0.4555	0.7551	116
117	-0.1285	-0.1415	-0.4581	-0.5192	0.6924	117
118	-0.0839	-0.1717	-0.2809	-0.5532	0.6204	118
119	-0.0437	-0.1830	-0.1433	-0.5610	0.5790	119
120	0.0	-0.1870	0.0	-0.5638	0.5638	120
121	-0.1544	0.0833	-0.7509	0.2948	0.8067	121
122	-0.1541	0.0595	-0.7680	0.1550	0.7835	122
123	-0.1550	0.0327	-0.7766	0.0189	0.7768	123
124	-0.1558	0.0038	-0.7577	-0.1235	0.7677	124
125	-0.1566	-0.0257	-0.7199	-0.2580	0.7647	125
126	-0.1511	-0.0615	-0.6509	-0.3920	0.7598	126
127	-0.1372	-0.1103	-0.5521	-0.5086	0.7507	127
128	-0.1116	-0.1592	-0.4198	-0.5923	0.7260	128
129	-0.0720	-0.1964	-0.2581	-0.6384	0.6886	129
130	-0.0377	-0.2117	-0.1318	-0.6534	0.6666	130
131	0.0	-0.2166	0.0	-0.6572	0.6572	131
132	-0.1409	0.0594	-0.6868	0.1863	0.7116	132
133	-0.1402	0.0329	-0.6907	0.0410	0.6919	133
134	-0.1410	0.0044	-0.6852	-0.1068	0.6935	134
135	-0.1403	-0.0265	-0.6473	-0.2608	0.6979	135
136	-0.1349	-0.0665	-0.5865	-0.4100	0.7156	136
137	-0.1214	-0.1196	-0.4958	-0.5464	0.7378	137
138	-0.0977	-0.1751	-0.3772	-0.6463	0.7484	138
139	-0.0627	-0.2184	-0.2321	-0.7071	0.7442	139
140	-0.0325	-0.2364	-0.1187	-0.7270	0.7366	140
141	0.0	-0.2426	0.0	-0.7341	0.7341	141
142	-0.1254	0.0325	-0.5760	0.0801	0.5815	142
143	-0.1243	0.0047	-0.5696	-0.0732	0.5743	143
144	-0.1235	-0.0277	-0.5506	-0.2338	0.5982	144
145	-0.1183	-0.0708	-0.4980	-0.4024	0.6403	145
146	-0.1067	-0.1283	-0.4231	-0.5540	0.6971	146
147	-0.0853	-0.1897	-0.3214	-0.6740	0.7467	147
148	-0.0540	-0.2377	-0.1981	-0.7469	0.7727	148
149	-0.0278	-0.2581	-0.1011	-0.7748	0.7814	149
150	0.0	-0.2648	0.0	-0.7827	0.7827	150
151	-0.1073	0.0043	-0.4300	-0.0199	0.4305	151
152	-0.1048	-0.0288	-0.4151	-0.1809	0.4528	152
153	-0.1009	-0.0743	-0.3860	-0.3528	0.5229	153
154	-0.0913	-0.1358	-0.3255	-0.5220	0.6151	154
155	-0.0726	-0.2030	-0.2470	-0.6552	0.7002	155
156	-0.0448	-0.2548	-0.1507	-0.7439	0.7590	156
157	-0.0229	-0.2763	-0.0771	-0.7763	0.7801	157
158	0.0	-0.2839	0.0	-0.7882	0.7882	158
159	-0.0828	-0.0300	-0.2665	-0.1060	0.2868	159
160	-0.0798	-0.0766	-0.2477	-0.2714	0.3674	160
161	-0.0741	-0.1416	-0.2152	-0.4376	0.4877	161
162	-0.0581	-0.2154	-0.1579	-0.5811	0.6022	162
163	-0.0345	-0.2692	-0.0945	-0.6732	0.6798	163
164	-0.0166	-0.2915	-0.0473	-0.7115	0.7131	164
165	0.0	-0.2982	0.0	-0.7225	0.7225	165
166	-0.0539	-0.0780	-0.1177	-0.1634	0.2014	166
167	-0.0518	-0.1443	-0.1012	-0.3111	0.3272	167
168	-0.0410	-0.2269	-0.0764	-0.4381	0.4447	168
169	-0.0206	-0.2810	-0.0403	-0.5238	0.5254	169
170	-0.0106	-0.3013	-0.0197	-0.5549	0.5553	170
171	0.0	-0.3093	0.0	-0.5674	0.5674	171
172	-0.0245	-0.1455	-0.0245	-0.1455	0.1476	172
173	-0.0138	-0.2373	-0.0138	-0.2373	0.2377	173
174	-0.0073	-0.2861	-0.0073	-0.2861	0.2862	174

175	-0.0029	-0.3083	-0.0029	-0.3083	0.3083	175
176	0.0	-0.3140	0.0	-0.3140	0.3140	176
177	0.0	0.0	0.0	0.0	0.0	177
178	0.0	0.0	0.0	0.0	0.0	178
179	0.0	0.0	0.0	0.0	0.0	179
180	0.0	0.0	0.0	0.0	0.0	180

STRESSES AND STRESS LEVELS FOR FINAL CONDITION AT END OF INCREMENT

ELE	SIG-X	SIG-Y	TAU-XY	SIG-1	SIG-3	TAU-MAX	THETA	SIG1/SIG3	SLMAX	SLPRES	ELE
1	3.050	2.961	0.040	3.065	2.946	0.060	69.163	1.040	0.092	0.092	1
2	3.048	2.962	0.112	3.125	2.885	0.120	55.457	1.083	0.186	0.186	2
3	3.024	2.936	0.176	3.161	2.799	0.181	52.062	1.130	0.281	0.281	3
4	3.012	2.899	0.240	3.201	2.709	0.246	51.623	1.182	0.381	0.381	4
5	2.967	2.789	0.315	3.206	2.551	0.327	52.882	1.257	0.507	0.507	5
6	3.043	2.795	0.403	3.341	2.497	0.422	53.541	1.338	0.653	0.653	6
7	3.162	2.902	0.481	3.530	2.533	0.498	52.563	1.393	0.771	0.771	7
8	3.398	3.177	0.531	3.830	2.745	0.542	50.872	1.395	0.839	0.839	8
9	3.569	3.441	0.568	4.076	2.934	0.571	48.228	1.389	0.884	0.884	9
10	3.882	3.871	0.587	4.464	3.289	0.587	45.266	1.357	0.909	0.909	10
11	4.186	4.283	0.590	4.826	3.643	0.592	42.656	1.325	0.916	0.916	11
12	4.666	4.847	0.580	5.344	4.169	0.587	40.567	1.282	0.909	0.909	12
13	5.254	5.506	0.562	5.956	4.804	0.576	38.683	1.240	0.891	0.891	13
14	5.810	6.116	0.533	6.517	5.409	0.554	36.995	1.205	0.858	0.858	14
15	6.184	6.531	0.493	6.880	5.835	0.522	35.298	1.179	0.809	0.809	15
16	6.528	6.910	0.433	7.192	6.246	0.473	33.112	1.152	0.732	0.732	16
17	6.755	7.174	0.343	7.367	6.563	0.402	29.264	1.122	0.622	0.622	17
18	6.911	7.361	0.219	7.450	6.822	0.314	22.136	1.092	0.486	0.486	18
19	6.961	7.424	0.081	7.438	6.947	0.246	9.660	1.071	0.380	0.380	19
20	2.557	2.259	0.040	2.562	2.254	0.154	82.465	1.137	0.238	0.238	20
21	2.552	2.255	0.116	2.592	2.215	0.189	71.006	1.170	0.292	0.292	21
22	2.562	2.253	0.182	2.646	2.168	0.239	65.141	1.220	0.370	0.370	22
23	2.564	2.176	0.238	2.677	2.062	0.307	64.585	1.298	0.476	0.476	23
24	2.670	2.118	0.282	2.789	1.999	0.395	67.200	1.395	0.611	0.611	24
25	2.788	2.068	0.318	2.909	1.948	0.481	69.275	1.493	0.744	0.744	25
26	3.040	2.265	0.362	3.183	2.122	0.530	68.482	1.500	0.821	0.821	26
27	3.182	2.441	0.407	3.362	2.261	0.551	66.133	1.487	0.852	0.852	27
28	3.414	2.826	0.456	3.662	2.577	0.542	61.422	1.421	0.840	0.840	28
29	3.505	3.154	0.475	3.836	2.823	0.506	55.140	1.359	0.784	0.784	29
30	3.762	3.729	0.409	4.155	3.336	0.409	46.137	1.245	0.634	0.634	30
31	4.034	4.134	0.339	4.427	3.741	0.343	40.818	1.183	0.578	0.531	31
32	4.422	4.891	0.289	5.029	4.284	0.373	25.482	1.174	0.605	0.577	32
33	4.791	5.418	0.293	5.534	4.676	0.429	21.555	1.184	0.664	0.664	33
34	5.225	5.915	0.291	6.022	5.118	0.452	20.076	1.177	0.699	0.699	34
35	5.528	6.254	0.273	6.345	5.437	0.454	18.453	1.167	0.703	0.703	35
36	5.823	6.583	0.219	6.642	5.764	0.439	14.993	1.152	0.679	0.679	36
37	5.988	6.770	0.141	6.795	5.963	0.416	9.888	1.139	0.644	0.644	37
38	6.079	6.870	0.050	6.873	6.076	0.398	3.605	1.131	0.617	0.617	38
39	1.911	1.614	0.040	1.916	1.609	0.153	82.538	1.191	0.260	0.260	39
40	1.920	1.624	0.115	1.959	1.584	0.187	71.043	1.237	0.319	0.319	40
41	1.914	1.608	0.181	1.998	1.524	0.237	65.060	1.311	0.410	0.410	41
42	1.932	1.584	0.224	2.041	1.475	0.283	63.962	1.385	0.496	0.496	42
43	1.943	1.479	0.229	2.038	1.384	0.327	67.688	1.472	0.585	0.585	43
44	2.121	1.494	0.219	2.190	1.425	0.383	72.530	1.537	0.678	0.678	44
45	2.329	1.586	0.232	2.396	1.520	0.438	73.987	1.576	0.758	0.758	45
46	2.658	1.886	0.290	2.754	1.789	0.483	71.556	1.539	0.784	0.784	46
47	2.773	2.136	0.364	2.938	1.971	0.484	65.570	1.491	0.755	0.755	47
48	3.060	2.618	0.374	3.273	2.405	0.434	60.266	1.361	0.619	0.619	48
49	3.277	3.153	0.271	3.492	2.937	0.278	51.432	1.189	0.357	0.357	49
50	3.602	3.587	0.201	3.795	3.394	0.201	46.040	1.118	0.326	0.239	50
51	3.805	4.256	0.129	4.291	3.771	0.260	14.974	1.138	0.397	0.291	51
52	4.069	4.883	0.153	4.911	4.041	0.435	10.274	1.215	0.472	0.467	52
53	4.202	5.252	0.147	5.272	4.181	0.545	7.799	1.261	0.573	0.573	53
54	4.440	5.693	0.146	5.710	4.424	0.643	6.579	1.291	0.653	0.653	54
55	4.609	5.986	0.113	5.996	4.600	0.698	4.649	1.303	0.691	0.691	55
56	4.767	6.224	0.064	6.227	4.764	0.731	2.530	1.307	0.708	0.708	56

57	4.821	6.310	0.022	6.310	4.820	0.745	0.842	1.309	0.716	0.716	57
58	2.754	0.956	0.029	2.754	0.956	0.899	89.077	2.881	0.633	0.633	58
59	2.815	0.959	0.093	2.820	0.954	0.933	87.127	2.956	0.657	0.657	59
60	2.928	0.966	0.155	2.941	0.954	0.994	85.502	3.084	0.699	0.699	60
61	3.038	0.934	0.200	3.057	0.915	1.071	84.621	3.340	0.754	0.754	61
62	3.176	0.910	0.176	3.190	0.897	1.147	85.587	3.558	0.807	0.807	62
63	3.285	0.863	0.100	3.289	0.859	1.215	87.646	3.829	0.855	0.855	63
64	3.546	1.054	0.080	3.549	1.052	1.248	88.166	3.373	0.878	0.878	64
65	3.668	1.190	0.139	3.676	1.182	1.247	86.789	3.110	0.878	0.878	65
66	3.942	1.692	0.356	3.997	1.637	1.180	81.210	2.442	0.830	0.830	66
67	3.705	1.956	0.349	3.772	1.888	0.942	79.115	1.997	0.663	0.663	67
68	3.574	2.537	0.344	3.677	2.433	0.622	73.240	1.511	0.438	0.438	68
69	2.889	2.913	0.253	3.155	2.648	0.253	43.653	1.191	0.523	0.178	69
70	2.467	3.695	0.197	3.725	2.437	0.644	8.880	1.529	0.652	0.453	70
71	2.125	4.195	0.104	4.201	2.120	1.040	2.874	1.981	0.749	0.732	71
72	2.351	4.687	0.035	4.688	2.351	1.168	0.867	1.994	0.822	0.822	72
73	2.591	5.047	0.018	5.047	2.591	1.228	0.426	1.948	0.864	0.864	73
74	2.914	5.419	0.000	5.419	2.914	1.252	0.002	1.859	0.881	0.881	74
75	3.087	5.613	-0.008	5.613	3.087	1.263	-0.182	1.818	0.889	0.889	75
76	3.180	5.716	-0.004	5.716	3.180	1.268	-0.101	1.797	0.892	0.892	76
77	1.283	0.311	0.011	1.283	0.311	0.486	89.361	4.126	0.266	0.266	77
78	1.371	0.311	0.035	1.372	0.310	0.531	88.132	4.430	0.290	0.290	78
79	1.556	0.307	0.065	1.560	0.303	0.628	87.049	5.144	0.343	0.343	79
80	1.844	0.310	0.084	1.848	0.305	0.772	86.863	6.057	0.422	0.422	80
81	2.157	0.312	0.076	2.160	0.308	0.926	87.648	7.001	0.506	0.506	81
82	2.410	0.325	0.021	2.411	0.325	1.043	89.419	7.414	0.568	0.568	82
83	2.500	0.316	-0.012	2.500	0.316	1.092	-89.692	7.920	0.596	0.596	83
84	2.677	0.552	0.154	2.688	0.541	1.074	85.880	4.968	0.568	0.568	84
85	2.201	0.624	0.354	2.277	0.549	0.864	77.920	4.150	0.457	0.457	85
86	2.625	1.667	0.379	2.757	1.535	0.611	70.823	1.797	0.286	0.286	86
87	2.062	1.611	0.497	2.382	1.291	0.546	57.223	1.845	0.263	0.263	87
88	2.261	2.657	0.448	2.949	1.969	0.490	33.094	1.498	0.268	0.218	88
89	1.881	3.006	0.349	3.105	1.781	0.662	15.916	1.743	0.318	0.301	89
90	1.841	3.781	0.139	3.790	1.831	0.980	4.084	2.070	0.443	0.443	90
91	1.623	3.999	0.002	3.999	1.623	1.188	0.046	2.465	0.550	0.550	91
92	1.672	4.476	-0.077	4.478	1.670	1.404	-1.571	2.682	0.646	0.646	92
93	1.705	4.745	-0.087	4.747	1.702	1.522	-1.632	2.789	0.698	0.698	93
94	1.802	4.983	-0.073	4.985	1.800	1.592	-1.314	2.769	0.722	0.722	94
95	1.823	5.054	-0.025	5.054	1.823	1.616	-0.448	2.773	0.731	0.731	95
96	1.405	0.603	0.280	1.493	0.514	0.490	72.524	2.904	0.108	0.108	96
97	0.927	0.454	0.416	1.169	0.212	0.479	59.798	5.526	0.108	0.108	97
98	1.641	1.513	0.408	1.990	1.164	0.413	49.450	1.709	0.093	0.087	98
99	1.443	1.712	0.449	2.046	1.109	0.468	36.653	1.845	0.102	0.099	99
100	1.830	2.707	0.374	2.845	1.692	0.576	20.209	1.681	0.120	0.117	100
101	1.567	3.092	0.252	3.132	1.527	0.803	9.153	2.052	0.164	0.164	101
102	1.349	3.600	0.111	3.606	1.344	1.131	2.817	2.684	0.235	0.235	102
103	0.965	3.822	-0.017	3.822	0.965	1.429	-0.347	3.961	0.305	0.305	103
104	0.806	4.163	-0.074	4.165	0.804	1.680	-1.257	5.180	0.363	0.363	104
105	0.679	4.300	-0.071	4.301	0.677	1.812	-1.121	6.352	0.395	0.395	105
106	0.660	4.404	-0.028	4.404	0.660	1.872	-0.421	6.674	0.408	0.408	106
107	0.627	0.340	0.183	0.724	0.253	0.236	64.601	2.862	0.060	0.053	107
108	0.672	0.531	0.266	0.876	0.326	0.275	52.421	2.688	0.065	0.062	108
109	1.305	1.440	0.325	1.705	1.040	0.332	39.110	1.639	0.080	0.070	109
110	1.123	1.890	0.356	2.030	0.983	0.523	21.403	2.065	0.112	0.111	110
111	1.298	2.701	0.337	2.778	1.222	0.778	12.833	2.274	0.163	0.163	111
112	1.021	2.963	0.250	2.994	0.989	1.002	7.229	3.026	0.213	0.213	112
113	0.891	3.379	0.102	3.383	0.886	1.248	2.349	3.817	0.268	0.268	113
114	0.659	3.538	0.000	3.538	0.659	1.440	0.007	5.367	0.314	0.314	114
115	0.591	3.732	-0.031	3.732	0.591	1.571	-0.570	6.317	0.345	0.345	115
116	0.533	3.765	-0.013	3.765	0.533	1.616	-0.238	7.065	0.356	0.356	116

117	0.367	0.232	0.057	0.388	0.211	0.088	69.827	1.834	0.032	0.020	117
118	0.481	0.529	0.166	0.673	0.337	0.168	40.831	1.998	0.052	0.038	118
119	1.010	1.541	0.300	1.676	0.874	0.401	24.257	1.917	0.087	0.086	119
120	0.826	1.899	0.359	2.008	0.717	0.645	16.889	2.800	0.140	0.140	120
121	0.940	2.578	0.322	2.639	0.879	0.880	10.743	3.003	0.189	0.189	121
122	0.716	2.762	0.195	2.781	0.698	1.041	5.407	3.986	0.227	0.227	122
123	0.635	3.052	0.068	3.054	0.633	1.210	1.603	4.824	0.265	0.265	123
124	0.504	3.101	0.013	3.101	0.504	1.299	0.281	6.154	0.287	0.287	124
125	0.487	3.179	-0.001	3.179	0.487	1.346	-0.024	6.523	0.298	0.298	125
126	0.114	0.147	-0.060	0.193	0.069	0.062	-37.239	2.813	0.019	0.014	126
127	0.339	0.625	0.160	0.697	0.267	0.215	24.137	2.610	0.050	0.048	127
128	0.778	1.519	0.317	1.637	0.661	0.488	20.295	2.476	0.106	0.106	128
129	0.634	1.830	0.344	1.921	0.542	0.690	14.941	3.546	0.152	0.152	129
130	0.725	2.362	0.252	2.400	0.687	0.856	8.565	3.491	0.186	0.186	130
131	0.567	2.440	0.124	2.448	0.559	0.944	3.772	4.379	0.208	0.208	131
132	0.550	2.588	0.048	2.589	0.549	1.020	1.335	4.719	0.225	0.225	132
133	0.492	2.576	0.014	2.576	0.492	1.042	0.384	5.240	0.230	0.230	133
134	-0.015	0.174	-0.079	0.203	-0.044	0.123	-20.078	-4.653	0.028	0.028	134
135	0.324	0.650	0.198	0.743	0.231	0.256	25.237	3.221	0.058	0.058	135
136	0.659	1.450	0.305	1.554	0.555	0.500	18.825	2.802	0.110	0.110	136
137	0.547	1.667	0.268	1.728	0.486	0.621	12.776	3.553	0.137	0.137	137
138	0.651	1.998	0.148	2.014	0.635	0.690	6.191	3.174	0.151	0.151	138
139	0.574	1.968	0.073	1.971	0.570	0.701	2.980	3.459	0.154	0.154	139
140	0.601	2.029	0.018	2.029	0.601	0.714	0.733	3.377	0.157	0.157	140
141	0.014	0.178	0.012	0.179	0.013	0.083	4.130	14.102	0.019	0.019	141
142	0.352	0.662	0.197	0.757	0.257	0.250	25.879	2.949	0.056	0.056	142
143	0.632	1.277	0.224	1.347	0.562	0.392	17.392	2.396	0.086	0.086	143
144	0.577	1.350	0.137	1.373	0.554	0.410	9.754	2.481	0.090	0.090	144
145	0.725	1.496	0.057	1.500	0.721	0.390	4.191	2.081	0.085	0.085	145
146	0.700	1.440	0.023	1.441	0.699	0.371	1.776	2.060	0.081	0.081	146
147	0.159	0.195	0.072	0.251	0.102	0.074	38.001	2.459	0.017	0.017	147
148	0.381	0.583	0.140	0.654	0.310	0.172	27.085	2.111	0.039	0.039	148
149	0.632	0.919	0.052	0.928	0.623	0.153	9.924	1.490	0.033	0.033	149
150	0.613	0.837	0.045	0.846	0.604	0.121	10.816	1.400	0.026	0.026	150
151	0.677	0.896	0.011	0.896	0.677	0.110	2.858	1.324	0.024	0.024	151
152	0.143	0.149	0.033	0.179	0.112	0.033	42.494	1.594	0.008	0.008	152
153	0.286	0.297	0.0	0.297	0.286	0.006	0.0	1.041	0.001	0.001	153
154	0.286	0.297	0.0	0.297	0.286	0.006	0.0	1.041	0.001	0.001	154
155	0.286	0.297	0.0	0.297	0.286	0.006	0.0	1.041	0.001	0.001	155

SOLUTION TIME

FORM ELEMENT STIFFNESSES********** 0.0

FORM TOTAL STIFFNESS************** 0.0

EQUATION SOLVING***************** 0.0

CALCULATE STRESSES AND STRAINS**** 0.0

SOLUTION TIME FOR THIS ITERATION** 0.0

DETERMINE CONTROL DATA************ 0.0

FORM LOAD VECTER***************** 0.0

TOTAL TIME FOR THIS LOAD CASE***** 0.0

APPENDIX D

SUPPORTING DATA FOR THE FINITE ELEMENT COMPUTER PROGRAM

MODULUS AND POISSON'S RATIO VALUES BASED ON AVERAGE STRESSES DURING THE INCREMENT
STRAINS FOR FINAL CONDITION AT END OF INCREMENT

ELE	ELAS MOD	BULK MOD	SHEAR MOD	POIS	EPS-X	EPS-Y	GAM-XY	EPS-1	EPS-3	GAMMAX	ELE
1	117.0	1963.9	39.3	0.490	0.055	-0.047	0.091	0.072	-0.064	0.136	1
2	98.4	1651.2	33.0	0.490	0.059	-0.049	0.281	0.155	-0.146	0.301	2
3	81.5	1367.7	27.4	0.490	0.066	-0.057	0.485	0.255	-0.246	0.500	3
4	64.8	1087.0	21.7	0.490	0.093	-0.085	0.743	0.386	-0.378	0.764	4
5	46.3	776.4	15.5	0.490	0.171	-0.167	1.156	0.604	-0.601	1.205	5
6	26.0	436.5	8.7	0.490	0.325	-0.315	1.969	1.040	-1.030	2.070	6
7	12.8	215.1	4.3	0.490	0.521	-0.497	3.374	1.774	-1.750	3.524	7
8	6.9	115.6	2.3	0.490	0.749	-0.669	5.243	2.756	-2.675	5.432	8
9	4.0	67.9	1.4	0.490	0.915	-0.833	7.771	4.024	-3.941	7.965	9
10	2.7	45.3	0.9	0.490	0.882	-0.774	10.910	5.572	-5.463	11.035	10
11	2.2	36.7	0.7	0.490	0.534	-0.465	13.277	6.692	-6.623	13.315	11
12	2.1	34.6	0.7	0.490	0.038	0.180	14.425	7.322	-7.104	14.426	12
13	2.2	37.5	0.8	0.490	-0.335	1.139	13.923	7.402	-6.599	14.001	13
14	2.9	48.2	1.0	0.490	-0.662	1.741	12.053	6.684	-5.606	12.290	14
15	4.2	69.7	1.4	0.490	-0.821	1.831	9.482	5.428	-4.418	9.846	15
16	6.5	109.8	2.2	0.490	-0.813	1.680	6.716	4.016	-3.148	7.163	16
17	10.9	183.1	3.7	0.490	-0.757	1.453	4.098	2.676	-1.980	4.656	17
18	17.3	290.5	5.8	0.490	-0.659	1.236	2.047	1.683	-1.106	2.789	18
19	23.1	387.2	7.7	0.490	-0.585	1.099	0.654	1.160	-0.647	1.807	19
20	116.9	1960.8	39.2	0.490	0.151	-0.141	0.080	0.157	-0.147	0.303	20
21	104.8	1758.2	35.2	0.490	0.160	-0.150	0.244	0.202	-0.192	0.394	21
22	87.4	1466.7	29.3	0.490	0.182	-0.171	0.420	0.280	-0.269	0.549	22
23	67.0	1124.8	22.5	0.490	0.261	-0.250	0.628	0.411	-0.400	0.810	23
24	41.7	700.0	14.0	0.490	0.469	-0.453	0.949	0.670	-0.654	1.323	24
25	21.6	362.1	7.2	0.490	0.848	-0.825	1.521	1.142	-1.119	2.261	25
26	11.3	190.2	3.8	0.490	1.311	-1.245	2.465	1.808	-1.743	3.551	26
27	8.1	136.1	2.7	0.490	1.668	-1.590	3.267	2.346	-2.267	4.613	27
28	8.0	134.1	2.7	0.490	1.814	-1.699	3.635	2.585	-2.470	5.055	28
29	11.4	191.7	3.8	0.490	1.514	-1.420	3.477	2.322	-2.228	4.549	29
30	19.1	321.0	6.4	0.490	0.800	-0.656	2.605	1.564	-1.420	2.984	30
31	320.2	5373.2	107.5	0.490	-0.052	0.234	2.113	1.157	-0.975	2.132	31
32	275.8	4627.3	92.5	0.490	-0.572	0.858	2.000	1.372	-1.086	2.459	32
33	11.5	193.2	3.9	0.490	-1.072	1.541	2.358	1.994	-1.525	3.519	33
34	9.3	155.7	3.1	0.490	-1.471	2.087	2.864	2.592	-1.975	4.567	34
35	8.9	149.0	3.0	0.490	-1.650	2.332	3.055	2.850	-2.168	5.019	35
36	9.7	163.2	3.3	0.490	-1.718	2.420	2.528	2.776	-2.074	4.849	36
37	11.1	186.9	3.7	0.490	-1.681	2.361	1.563	2.506	-1.826	4.333	37
38	12.2	204.8	4.1	0.490	-1.620	2.286	0.543	2.305	-1.639	3.943	38
39	67.5	1133.3	22.7	0.490	0.264	-0.249	0.138	0.273	-0.258	0.531	39
40	58.4	980.5	19.6	0.490	0.284	-0.267	0.432	0.358	-0.342	0.700	40
41	45.8	768.2	15.4	0.490	0.332	-0.315	0.770	0.512	-0.494	1.006	41
42	35.1	588.2	11.8	0.490	0.438	-0.418	1.088	0.702	-0.682	1.385	42
43	25.6	429.7	8.6	0.490	0.690	-0.672	1.298	0.949	-0.932	1.881	43
44	17.4	292.0	5.8	0.490	1.144	-1.105	1.524	1.378	-1.339	2.716	44
45	12.0	200.5	4.0	0.490	1.666	-1.601	1.932	1.930	-1.865	3.795	45
46	10.7	179.0	3.6	0.490	1.944	-1.829	2.403	2.294	-2.179	4.473	46
47	13.4	225.[illegible]	4.5	0.490	1.571	-1.478	2.525	2.026	-1.933	3.959	47
48	26.1	437.1	8.7	0.490	0.925	-0.828	1.855	1.324	-1.228	2.552	48
49	60.1	1008.9	20.2	0.490	0.292	-0.179	1.021	0.618	-0.506	1.124	49
50	418.8	7026.3	140.5	0.490	-0.183	0.308	0.659	0.474	-0.348	0.822	50
51	427.7	7175.7	143.5	0.490	-0.442	0.606	0.606	0.688	-0.523	1.211	51
52	435.2	7301.6	146.0	0.490	-0.735	0.954	0.603	1.006	-0.787	1.793	52
53	33.2	557.2	11.1	0.490	-1.189	1.471	0.567	1.501	-1.219	2.720	53
54	26.3	440.6	8.8	0.490	-1.634	1.962	0.694	1.995	-1.668	3.662	54
55	23.2	398.8	7.8	0.490	-1.941	2.295	0.584	2.315	-1.961	4.276	55

56	22.0	368.5	7.4	0.490	-2.126	2.502	0.328	2.508	-2.131	4.639	56
57	21.4	358.6	7.2	0.490	-2.211	2.596	0.115	2.597	-2.212	4.809	57
58	147.7	2478.7	49.6	0.490	0.356	-0.342	0.030	0.356	-0.342	0.698	58
59	129.4	2171.9	43.4	0.490	0.394	-0.378	0.106	0.397	-0.381	0.779	59
60	99.5	1669.1	33.4	0.490	0.476	-0.457	0.206	0.488	-0.468	0.956	60
61	67.0	1124.3	22.5	0.490	0.626	-0.602	0.345	0.650	-0.626	1.276	61
62	40.5	679.7	13.6	0.490	0.881	-0.847	0.446	0.909	-0.876	1.785	62
63	21.9	368.1	7.4	0.490	1.308	-1.262	0.529	1.335	-1.289	2.624	63
64	14.3	239.1	4.8	0.490	1.710	-1.632	0.688	1.745	-1.667	3.412	64
65	14.6	245.8	4.9	0.490	1.715	-1.648	0.442	1.730	-1.662	3.392	65
66	29.8	500.5	10.0	0.490	1.191	-1.131	0.313	1.201	-1.142	2.343	66
67	121.6	2040.5	40.8	0.490	0.456	-0.432	0.126	0.460	-0.437	0.897	67
68	298.7	5011.2	100.2	0.490	0.049	-0.032	0.113	0.078	-0.061	0.139	68
69	2742.0	46007.3	920.1	0.490	-0.169	0.187	0.164	0.205	-0.188	0.392	69
70	2802.6	47023.1	940.5	0.490	-0.364	0.397	0.189	0.408	-0.375	0.783	70
71	2860.5	47994.1	959.9	0.490	-0.633	0.720	0.156	0.725	-0.638	1.362	71
72	25.3	425.3	8.5	0.490	-1.055	1.246	-0.086	1.246	-1.056	2.303	72
73	15.3	256.8	5.1	0.490	-1.563	1.850	-0.235	1.854	-1.567	3.421	73
74	11.6	194.1	3.9	0.490	-1.925	2.320	-0.320	2.326	-1.931	4.257	74
75	10.0	167.2	3.3	0.490	-2.162	2.629	-0.330	2.634	-2.167	4.802	75
76	9.3	156.4	3.1	0.490	-2.281	2.788	-0.133	2.788	-2.282	5.071	76
77	143.5	2408.4	48.2	0.490	0.397	-0.381	0.018	0.397	-0.381	0.778	77
78	135.3	2270.4	45.4	0.490	0.447	-0.429	0.059	0.448	-0.430	0.878	78
79	118.2	1982.7	39.7	0.490	0.566	-0.544	0.119	0.569	-0.547	1.117	79
80	95.7	1606.1	32.1	0.490	0.779	-0.749	0.174	0.784	-0.754	1.538	80
81	74.5	1250.0	25.0	0.490	1.076	-1.034	0.188	1.080	-1.038	2.119	81
82	60.9	1022.6	20.5	0.490	1.363	-1.309	0.085	1.364	-1.310	2.673	82
83	54.8	919.5	18.4	0.490	1.530	-1.469	0.017	1.530	-1.469	2.999	83
84	68.7	1152.3	23.0	0.490	1.306	-1.244	0.297	1.315	-1.253	2.568	84
85	102.1	1713.0	34.3	0.490	0.795	-0.759	0.503	0.835	-0.799	1.634	85
86	197.1	3307.2	66.1	0.490	0.378	-0.332	0.424	0.437	-0.391	0.827	86
87	1049.3	17605.2	352.1	0.490	0.028	0.004	0.631	0.332	-0.300	0.632	87
88	1152.5	19336.4	386.7	0.490	-0.151	0.197	0.573	0.358	-0.312	0.671	88
89	1137.5	19085.5	381.7	0.490	-0.352	0.401	0.448	0.463	-0.413	0.876	89
90	1146.1	19229.8	384.6	0.490	-0.627	0.693	0.251	0.705	-0.639	1.344	90
91	87.0	1460.3	29.2	0.490	-1.039	1.121	0.013	1.121	-1.039	2.159	91
92	61.2	1027.4	20.5	0.490	-1.487	1.588	-0.222	1.592	-1.491	3.082	92
93	49.5	829.9	16.6	0.490	-1.831	1.945	-0.295	1.951	-1.837	3.788	93
94	44.9	752.8	15.1	0.490	-2.041	2.167	-0.261	2.171	-2.045	4.216	94
95	43.2	725.2	14.5	0.490	-2.128	2.258	-0.096	2.259	-2.128	4.387	95
96	127.5	2139.8	42.8	0.490	0.559	-0.513	0.714	0.667	-0.621	1.288	96
97	105.4	1769.1	35.4	0.490	0.313	-0.294	0.982	0.586	-0.568	1.154	97
98	550.9	9244.0	184.9	0.490	0.059	-0.010	0.793	0.422	-0.373	0.796	98
99	546.5	9169.2	183.4	0.490	-0.149	0.198	0.792	0.457	-0.408	0.865	99
100	609.0	10218.8	204.4	0.490	-0.364	0.434	0.628	0.543	-0.473	1.015	100
101	159.5	2676.2	53.5	0.490	-0.645	0.720	0.454	0.756	-0.681	1.438	101
102	144.5	2424.4	48.5	0.490	-1.000	1.081	0.225	1.088	-1.006	2.094	102
103	124.0	2080.9	41.6	0.490	-1.368	1.448	-0.001	1.448	-1.368	2.816	103
104	112.9	1894.6	37.9	0.490	-1.682	1.764	-0.118	1.765	-1.683	3.448	104
105	106.3	1783.2	35.7	0.490	-1.873	1.955	-0.129	1.957	-1.874	3.831	105
106	104.6	1755.0	35.1	0.490	-1.953	2.037	-0.051	2.037	-1.953	3.990	106
107	365.2	6127.1	122.5	0.490	0.228	-0.208	0.485	0.336	-0.316	0.652	107
108	396.7	6656.5	133.1	0.490	0.097	-0.081	0.645	0.342	-0.327	0.669	108
109	537.7	9021.5	180.4	0.490	-0.094	0.137	0.652	0.367	-0.325	0.692	109
110	151.8	2546.6	50.9	0.490	-0.347	0.395	0.693	0.532	-0.483	1.015	110
111	152.7	2562.4	51.2	0.490	-0.621	0.686	0.627	0.757	-0.692	1.449	111
112	138.0	2314.6	46.3	0.490	-0.914	0.981	0.514	1.015	-0.949	1.964	112
113	127.4	2137.0	42.7	0.490	-1.224	1.297	0.254	1.304	-1.231	2.534	113
114	114.0	1912.3	38.2	0.490	-1.506	1.579	0.053	1.580	-1.506	3.086	114
115	108.4	1819.5	36.4	0.490	-1.686	1.762	-0.032	1.762	-1.686	3.448	115

116	105.2	1764.7	35.3	0.490	-1.764	1.840	-0.017	1.840	-1.764	3.604	116
117	356.5	5980.9	119.6	0.490	0.115	-0.105	0.193	0.152	-0.141	0.293	117
118	397.7	6672.8	133.5	0.490	-0.018	0.030	0.495	0.255	-0.243	0.497	118
119	152.6	2560.0	51.2	0.490	-0.241	0.281	0.589	0.414	-0.374	0.788	119
120	136.8	2295.4	45.9	0.490	-0.522	0.566	0.737	0.679	-0.635	1.314	120
121	138.9	2331.1	46.6	0.490	-0.785	0.844	0.658	0.908	-0.849	1.756	121
122	126.6	2123.6	42.5	0.490	-1.048	1.109	0.452	1.132	-1.072	2.204	122
123	119.4	2003.6	40.1	0.490	-1.290	1.356	0.190	1.360	-1.293	2.653	123
124	111.2	1865.1	37.3	0.490	-1.449	1.515	0.060	1.515	-1.449	2.964	124
125	109.3	1833.8	36.7	0.490	-1.517	1.585	0.008	1.585	-1.517	3.102	125
126	334.8	5617.8	112.4	0.490	0.020	-0.016	0.008	0.020	-0.017	0.037	126
127	384.1	6445.2	128.9	0.490	-0.123	0.133	0.437	0.258	-0.248	0.507	127
128	141.1	2366.9	47.3	0.490	-0.358	0.394	0.646	0.513	-0.478	0.991	128
129	129.1	2165.8	43.3	0.490	-0.616	0.656	0.753	0.759	-0.719	1.478	129
130	132.8	2228.9	44.6	0.490	-0.835	0.888	0.551	0.931	-0.878	1.809	130
131	123.8	2076.9	41.5	0.490	-1.014	1.067	0.299	1.078	-1.025	2.103	131
132	121.0	2031.0	40.6	0.490	-1.129	1.186	0.122	1.188	-1.130	2.318	132
133	117.2	1966.7	39.3	0.490	-1.180	1.237	0.038	1.237	-1.180	2.417	133
134	258.8	4341.7	86.8	0.490	-0.049	0.051	-0.052	0.057	-0.056	0.113	134
135	116.1	1948.0	39.0	0.490	-0.185	0.194	0.474	0.308	-0.299	0.607	135
136	136.5	2289.6	45.8	0.490	-0.398	0.431	0.648	0.542	-0.510	1.052	136
137	129.6	2174.0	43.5	0.490	-0.596	0.632	0.604	0.702	-0.666	1.368	137
138	135.9	2279.9	45.6	0.490	-0.702	0.747	0.323	0.765	-0.720	1.484	138
139	131.4	2205.0	44.1	0.490	-0.747	0.791	0.164	0.795	-0.752	1.547	139
140	132.0	2215.2	44.3	0.490	-0.766	0.812	0.041	0.812	-0.767	1.579	140
141	284.5	4773.1	95.5	0.490	-0.064	0.064	0.030	0.066	-0.066	0.132	141
142	120.1	2014.4	40.3	0.490	-0.174	0.184	0.475	0.302	-0.292	0.595	142
143	141.8	2379.5	47.6	0.490	-0.324	0.352	0.473	0.427	-0.398	0.825	143
144	138.8	2329.3	46.6	0.490	-0.397	0.426	0.295	0.452	-0.423	0.875	144
145	146.2	2452.3	49.0	0.490	-0.380	0.415	0.116	0.419	-0.385	0.804	145
146	146.2	2452.7	49.1	0.490	-0.365	0.398	0.047	0.399	-0.366	0.765	146
147	98.5	1653.2	33.1	0.490	-0.022	0.024	0.118	0.064	-0.062	0.126	147
148	126.9	2128.9	42.6	0.490	-0.107	0.116	0.328	0.203	-0.194	0.396	148
149	141.5	2373.8	47.5	0.490	-0.135	0.155	0.109	0.165	-0.145	0.310	149
150	141.8	2378.5	47.6	0.490	-0.103	0.121	0.094	0.130	-0.112	0.242	150
151	144.4	2422.8	48.5	0.490	-0.096	0.117	0.023	0.117	-0.097	0.214	151
152	82.3	1381.0	27.6	0.490	0.0	0.0	0.0	0.0	0.0	0.0	152
153	317.6	5379.3	106.6	0.490	0.0	0.0	0.0	0.0	0.0	0.0	153
154	317.6	5329.3	106.6	0.490	0.0	0.0	0.0	0.0	0.0	0.0	154
155	317.6	5329.3	106.6	0.490	0.0	0.0	0.0	0.0	0.0	0.0	155

THE EFFECTS OF DESICCATION ON SOIL DEFORMATION

by

John D. Wineland

B. S., Kansas University
Lawrence, Kansas
1969

AN ABSTRACT OF A MASTERS THESIS

submitted in partial fulfillment of the

requirements for the degree

MASTER OF SCIENCE

Department of Civil Engineering

KANSAS STATE UNIVERSITY
Manhattan, Kansas

1979

ABSTRACT

Accurate prediction of the deformation or soil movement which occurs in the foundation of embankments is necessary because of the effect this deformation may have on drainage structures utility lines, etc. The effect of desiccation on the deformation of the foundation soils and its effect on the overall stability of embankments must be considered. A literature review of desiccation yielded information regarding the process of desiccation. However, very little information on changes in soil strength or the stress-strain characteristics resulting from desiccation was found.

Instrumentation was installed to monitor the stability and foundation deformation during construction of an embankment by the Kansas Department of Transportation. The actual foundation deformation was compared with predictions made by two finite element computer analyses. The first analysis did not consider the effects of desiccation and predicted deformations were far in excess of those actually measured. The second analysis did account for the increased strength near the ground surface which resulted from desiccation. Deformation predictions made during this analysis were much more accurate than those made without considering the effects of desiccation.

Stability analyses using circular arc form of failure were performed. According to these analyses, desiccation resulted in an increase of 25 percent in the computed factor of safety against sliding for the embankment analyzed.

Methods of recognizing the desiccated zone and accounting for its incrased strength in the analysis are presented.